receptors affect the TNFR2-mediated activities of TNF-α, which are essential for immune function. Therefore, these therapies also have the potential to cause serious side effects, such as an increased risk of reactivating infectious disease or lymphoma. It is hoped that these problems can be overcome by the use of TNFR1-specific agents that selectively inhibit TNF-α-bioactivity through TNFR1 without interfering with TNFR2.

We have developed a novel technology to produce TNF-α muteins which bind to independent TNFRs using a unique phage-display method [19–21]. Recently we succeeded in producing a novel TNFR1-selective antagonistic mutant TNF-α (R1antTNF) using phage-display [21]. We showed that R1antTNF displays exclusive TNFR1 selective binding, which leads to effective and selective inhibitory effects of TNFR1-mediated biological activity both in vitro and in vivo without affecting TNFR2-mediated bioactivity [21].

In this study, we examined the therapeutic effect of R1antTNF in acute hepatitis using two independent experimental models, induced by carbon tetrachloride (CCl_4) or concanavalin A (ConA). R1antTNF showed anti-inflammatory effect on both acute hepatitis models. Especially, in CCl_4-induced acute hepatitis, R1antTNF showed superior therapeutic effect compared to the common anti-TNF-α Ab. These results indicate that R1antTNF can be a clinically useful TNF-α antagonist for the treatment of inflammatory diseases such as hepatitis.

2. Materials and methods

2.1. Cytokines and antibodies

Recombinant human wild-type TNF-α (wtTNF-α) and R1antTNF were purified as previously described [21]. Briefly, recombinant TNF-α s produced in *Escherichia coli* BL21(DE3) were recovered from inclusion bodies, washed in Triton X-100 and then solubilized in 6 M guanidine–HCl, 0.1 M Tris–HCl, pH 8.0 and 2 mM EDTA. Solubilized protein at 10 mg/ml was reduced with 10 mg/ml dithioerythritol for 4 h at room temperature and refolded by 100-fold dilution in a refolding buffer; 100 mM Tris–HCl, 2 mM EDTA, 0.5 M arginine and oxidized glutathione (551 mg/l). After dialysis against 20 mM Tris–HCl pH 7.4, containing 100 mM urea, active trimeric proteins were purified by Q-Sepharose (GE Healthcare Bioscience, Tokyo, Japan) and MonoQ chromatography (GE Healthcare Bioscience). Additionally, size-exclusion chromatography (Superose 12; GE Healthcare Bioscience) was performed. The endotoxin level of the purified TNF-αs were determined to be <300 pg/mg. Anti-mouse TNF-α Ab (MP6-XT3) was purchased from BD Biosciences Pharmingen (Franklin Lakes, NJ).

2.2. Cell culture

HEp-2 cells (a human laryngeal squamous cell carcinoma cell line) were provided by Cell Resource Center for Biomedical Research (Tohoku University, Sendai, Japan) and were maintained in RPMI 1640 (Sigma–Aldrich Japan, Tokyo, Japan) supplemented with 10% FBS and antibiotics. PC60-hTNFR1(+) cells (a mouse-rat fusion hybridoma consisting of human TNFR1-expressing PC60 cells) were generously provided by Dr. Vandenabeele (University of Gent, Belgium) [22], and maintained in RPMI 1640 supplemented with 10% FBS, 1 mM sodium pyruvate, 5×10^{-5} M 2-ME, 3 mg/ml puromycin (Wako Pure Chemical Industries, Osaka, Japan) and 1% antibiotic cocktail.

2.3. Cytotoxicity assay

For the inhibition assay, human HEp-2 cells were cultured in the 96-well plates (4×10^4 cells/well) in the presence of a constant concentration of the human wtTNF-α (20 ng/ml) and a serial dilution of the R1antTNF with 100 μg/ml cycloheximide. After incubation for 18 h, cell survival was determined using the methylene blue assay as described previously [21].

2.4. PC60-hTNFR1(+) assay

PC60-hTNFR1(+) were cultured at 5×10^4 cells/well with IL-1β (2 ng/ml). To evaluate the inhibitory activity, serially diluted R1antTNF and human wtTNF-α (200 ng/ml) were added. After 24 h incubation, the amount of rat GM-CSF produced was quantified by ELISA according to the manufacturer's protocol (R&D Systems, Minneapolis, MN).

2.5. Mice

BALB/c mice (6-week-old females) were purchased from CLEA Japan (Tokyo, Japan). All experimental protocols for animal studies were in accordance with "*Principles of Laboratory Animal Care*" (National Institutes of Health publication no. 85-23, revised 1985) and our institutional guidelines.

2.6. Hepatitis model

In the CCl_4-induced hepatitis model, mice were injected intraperitoneally with CCl_4 at a dose of 0.1 ml/kg in corn oil (10 ml/kg). Control mice received only corn oil. In this model, serum TNF-α levels reached maximum levels 12 h after treatment with CCl_4. R1antTNF and anti-mouse TNF-α Ab were administered intravenously to each group at 12 h after CCl_4 administration. Blood samples were taken at 48 h after CCl_4 administration under light ether anesthesia. In the ConA-induced hepatitis model, mice were injected intravenously with ConA (0.4 mg/mouse). Anti-mouse TNF-α Ab or R1antTNF was injected intravenously at 1 h after administration of ConA. Blood samples were taken at 4 h after ConA administration under light ether anesthesia.

2.7. Measurement of serum ALT and cytokine concentrations

Serum ALT concentration was measured using a colorimetric test (Wako Pure Chemical Industries). Serum IL-2 and IL-6 were determined by sandwich ELISA kits (DuoSet ELISA Development Systems; R&D systems). Serum samples were accordingly diluted with 1% BSA in PBS and then applied to a capture antibody-coated immunoplate. All procedures were according to the manufacturer's protocol. The ELISA detection limit was 10 pg/ml.

2.8. Statistical analysis

Data are expressed as mean values ± SEM and were analyzed by the one-way ANOVA with Dunnett's post test was performed ($^*p < 0.05$ vs. control).

3. Results

3.1. Antagonistic effect of R1antTNF on wtTNF-α induced cytotoxicity and cytokine production

To confirm the potency of R1antTNF as an antagonist to the human TNFR1-specific bioactivity of wtTNF-α, we examined the inhibitory effect of R1antTNF on wtTNF-α induced cytotoxicity in HEp-2 cells. The cytotoxic activity of wtTNF-α was inhibited by R1antTNF in a dose-dependent manner. In particular, cell viability increased from 10% to 80% after treatment with R1antTNF at 3×10^5 ng/ml (Fig. 1A). R1antTNF alone showed almost no biolog-

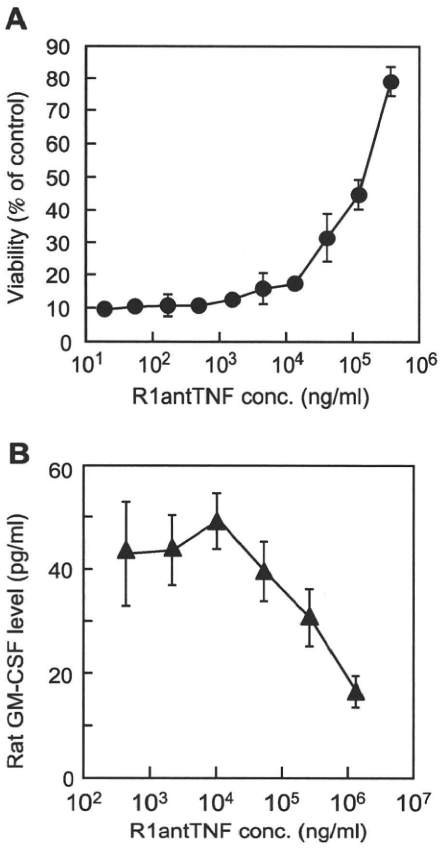

Fig. 1. Antagonistic activities of the R1antTNF. (A) Serial dilutions of R1antTNF were mixed with human wtTNF-α (20 ng/ml) and then applied to HEp-2 cells. After 18 h, the inhibitory effects of R1antTNF on the cytotoxicity of wtTNF-α were assessed by using the methylene blue assay. The absorbance of cells without wtTNF-α was plotted as 100 percent viability. (B) Serial dilutions of R1antTNF were mixed with human wtTNF-α (200 ng/ml) and applied to PC60-hTNFR1(+) cells (B). After 24 h, production of rat GM-CSF was quantified by ELISA. Rat GM-CSF was undetectable in the absence of wtTNF-α. The data represent the means ± SD ($n = 3$).

ical activity even when tested at 5×10^4 ng/ml (data not shown). We also confirmed the antagonistic effect of R1antTNF using another cell line. PC60-hTNFR1(+) cells, genetically engineered to express human TNFR1, were used to test the blocking activities of R1antTNF. R1antTNF efficiently inhibited wtTNF-α-mediated production of rat GM-CSF by PC60-hTNFR1(+) cells (Fig. 1B). The rat GM-CSF production mediated by wtTNF-α was not detected from PC60 cells, the parent cells of PC60-hTNFR1(+) cells. These results suggested that R1antTNF elicits an antagonistic effect against wtTNF-α through TNFR1.

3.2. Therapeutic effect of R1antTNF on hepatitis models

Firstly, we examined the therapeutic effect of R1antTNF in a CCl_4-induced hepatitis mouse model. CCl_4 is an industrial toxicant that is known to cause hepatic necrosis as well as free radical generation in kidney, heart, lung, testis, brain, and blood [23]. These reactive oxygen species can destroy cellular membranes, cellular proteins, and nucleic acids. The CCl_4-induced model has been extensively used as an experimental model of liver disease, such as hepatic cirrhosis and drug-induced hepatopathy. Injection of CCl_4-induced an accelerated serum ALT level, a well-characterized marker of liver damage. Treatment with R1antTNF, even at 30 μg/mouse, strongly inhibited elevation in the serum level of ALT (Fig.

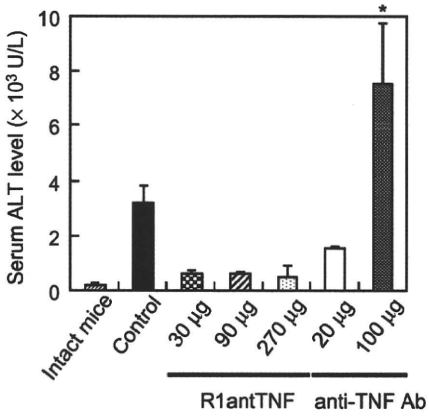

Fig. 2. Therapeutic effect of R1antTNF against the CCl_4-induced hepatitis model. BALB/c mice (6-week-old female) were intraperitoneally administered with CCl_4 at a dose of 0.1 ml/kg in corn oil (10 ml/kg). Intact animals received only corn oil. After 12 h, each mouse was given R1antTNF, anti-mouse TNF-α Ab, or PBS by intravenous injection. Blood samples were collected at 48 h after CCl_4 administration and serum ALT levels were then measured. Data represent the means ± SEM of three animals.

2). The serum level of ALT after treatment with R1antTNF at 30 μg/mouse was lower than that observed after treatment with anti-TNF-α Ab at 20 μg/mouse. Interestingly, treatment with the anti-TNF Ab at 100 μg/mouse actually raised the serum ALT levels compared to control mice, and seemed to even aggravate the hepatic disorder. These results indicate that R1antTNF may be more useful than anti-TNF-α Ab in treating CCl_4-induced hepatitis.

ConA-induced hepatitis in mice is a well-characterized model of T-cell-mediated liver disease and has been extensively used as a prototype mimicking human T-cell-mediated liver disease [24]. It is associated with elevated serum ALT, IL-2 and IL-6, and hepatic lesions are characterized by a massive granulocyte and T-cell infiltration, followed by hepatocyte necrosis and apoptosis. Thus, to examine the inhibitory effect of R1antTNF on Con A-induced activation of immune cells, we determined the elevation of serum IL-2 and IL-6. Initially, we examined the serum level of the T-cell-derived cytokine IL-2. R1antTNF dose-dependently reduced the level of serum IL-2 compared to control mice (Fig. 3A). The IL-2 level of mice treated with R1antTNF at 90 μg/mouse was the same as that of mice treated with anti-TNF-α Ab at 100 μg/mouse. Treatment with R1antTNF at 270 μg/mouse resulted in an even greater reduction in the serum level of IL-2. Next, to determine the inhibitory effect of R1antTNF on macrophage activation, we examined the serum IL-6 level, which is predominantly produced by Kupffer cells [25,26]. As with IL-2, R1antTNF dose-dependently reduced the serum level of IL-6 compared to control mice (Fig. 3B). The therapeutic effect thought to result from that R1antTNF inhibited ConA-induced activation of T-cells and macrophages as effectively as anti-TNF-α Ab.

4. Discussion

Previously we generated R1antTNF, a novel TNFR1-selective antagonistic mutant of TNF-α. The antagonistic effect of R1antTNF was demonstrated in vivo using a D-(+)-galactosamine (GalN)/TNF-α-dependent acute inflammatory liver injury model [21]. In this study, to clarify the therapeutic potency of R1antTNF more precisely, we examined the therapeutic effect of R1antTNF in two hepatitis models and compared the therapeutic efficacy to that of anti-TNF-α Ab.

In CCl_4-induced hepatitis model, previous study indicated that inflammatory cell influx, induction of adherent molecules in the li-

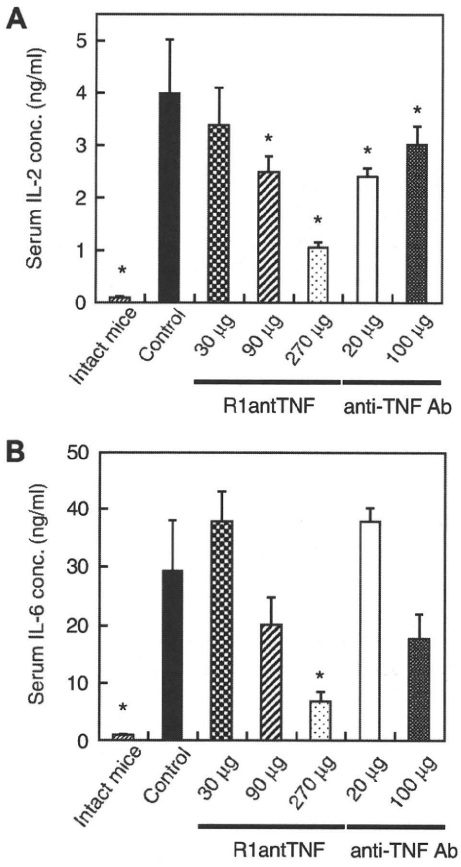

Fig. 3. Therapeutic effect of R1antTNF against ConA-induced hepatitis model. BALB/c mice (6-week-old female) were injected intravenously with ConA (0.4 mg/mouse). Anti-mouse TNF-α Ab or R1antTNF was injected 1 h after ConA injection. Blood samples were collected at 4 h after ConA injection. The serum IL-2 (A) and IL-6 (B) concentration was measured by ELISA ($n = 6$). Data represent the means ± SEM.

ver and serum ALT levels were decreased in TNFR1 knockout mice. In agreement with this, R1antTNF treatment clearly inhibited the elevation of ALT levels. However, remarkably when we used anti-TNF-α Ab as a reference for the efficacy of R1antTNF, we observed that administration of anti-TNF-α Ab increased ALT levels and even exacerbated liver failure, suggesting a paradoxical tissue protective effect of TNF-α. Similar observations were reported in a previous study, which reported that TNF-α induces the early-immediate inflammatory response through TNFR1 [27]. Additionally, it was reported that TNF-α plays an important role in the recovery from CCl_4-induced hepatitis through TNFR2 [28]. Thus, treatment with anti-TNF-α Ab may lead to adverse effects due to the lack of receptor-subtype specificity. These results indicate that R1antTNF may be more useful than anti-TNF-α Ab in treating TNFR1-dependent inflammatory diseases.

T-cell-mediated immune responses play a central role in hepatocellular injury induced by autoimmune hepatitis, viral infection, alcohol consumption, and hepatotoxins [29,30]. For example, $CD4^+$ T-cells are the predominant population of T-cells infiltrating into the liver in human autoimmune liver disease [31]. Therefore, we examined the therapeutic effect of R1antTNF on ConA-induced hepatitis model. R1antTNF inhibited the elevation of IL-2 and IL-6, which is mainly secreted from activated T-cells and Kupffer cells respectively. The therapeutic effect of R1antTNF on ConA-induced hepatitis model is almost the same as that of anti-TNF-α Ab. Numerous reports have shown that treatment with LPS or TNF-α in conjunction with D-galactosamine results in acute liver apoptosis and liver failure predominantly through TNFR1, resulting in activation of caspases and subsequent hepatocyte apoptosis [32,33]. However, studies by Kollias et al., and by Grell et al. have suggested that cell-associated TNF-α signaling through TNFR2 contributes to the development of rheumatoid arthritis and hepatocyte apoptosis [34–36]. Furthermore, investigators have argued that the liver injury from ConA treatment is not solely due to secreted TNF-α acting through TNFR1, but is also cell-associated TNF-α signaling through TNFR2 [35]. Thus, although the details of TNFR2-mediated signaling on hepatotoxicity are still unclear, it has been thought that the involvement of TNFR2 is different among hepatic models. Indeed, in our experiments, the treatment with anti-TNF-α Ab, which prevents TNF-α binding on both TNFR1 and TNFR2, exacerbated CCl_4-induced hepatitis model, but did not ConA-induced hepatitis model. Therefore, the fact that R1antTNF showed a substantial therapeutic effect in several hepatitis models is significant, and indicates the possibility that R1antTNF might be effective therapeutic agent for hepatitis caused by various factors.

One of the most common ways of enhancing the plasma half-lives of proteins is to conjugate them with polyethylene glycol (PEG) [37,38]. Because random introduction of PEG at the ε-amino groups of lysine residues usually lowers the bioactivity of proteins, application of PEGylation is generally limited to a small part of the protein. To overcome these problems of PEGylation, we recently developed a novel strategy for site-specific PEGylation via lysine-deficient mutant TNF-α, in which all of the lysine residues were replaced with other amino acids [19,20]. The lysine-deficient mutant TNF-α was site-specifically mono-PEGylated at its NH_2 terminus with PEG without loss of bioactivity. This site-specific mono-PEGylated mutant TNF-α showed increased in vivo therapeutic potency compared with the unmodified wtTNF-α and randomly mono-PEGylated wtTNF-α. R1antTNF was generated using a phage library based on this lysine-deficient mutant TNF-α and all of the lysine residues of R1antTNF were replaced with other amino acids [21]. We are currently attempting to construct mono-PEGylated R1antTNF. We anticipate that PEGylated R1antTNF will further enhance the anti-inflammatory activity for use in autoimmune disease models.

In conclusion, we have shown that R1antTNF is a useful TNF-α antagonist for treatment of hepatitis. Our results indicate that the therapeutic effect of R1antTNF can be equal or superior to that of anti-TNF-α Ab in treating TNFR1-dependent inflammatory diseases.

Acknowledgments

This study was supported in part by Grants-in-Aid for Scientific Research from the Ministry of Education, Culture, Sports, Science and Technology of Japan and Japan Society for the Promotion of Science (JSPS), in part by Health Labour Sciences Research Grant from the Ministry of Health, Labor and Welfare of Japan, in part by Health Sciences Research Grants for Research on Health Sciences focusing on Drug Innovation from the Japan Health Sciences Foundation, and in part by JSPS Research Fellowships for Young Scientists from the Japan Society for the Promotion of Science.

References

[1] Galun E, Axelrod JH. The role of cytokines in liver failure and regeneration: potential new molecular therapies. Biochim Biophys Acta 2002;1592:345–58.
[2] Vaquero J, Blei AT. Etiology and management of fulminant hepatic failure. Curr Gastroenterol Rep 2003;5:39–47.
[3] Lee WM. Acute liver failure in the United States. Semin Liver Dis 2003;23:217–26.
[4] Tracey KJ, Cerami A. Tumor necrosis factor: a pleiotropic cytokine and therapeutic target. Annu Rev Med 1994;45:491–503.

[5] Aggarwal BB. Signalling pathways of the TNF superfamily: a double-edged sword. Nat Rev Immunol 2003;3:745–56.
[6] Muto Y, Nouri-Aria KT, Meager A, Alexander GJ, Eddleston AL, Williams R. Enhanced tumour necrosis factor and interleukin-1 in fulminant hepatic failure. Lancet 1988;2:72–4.
[7] Bird GL, Sheron N, Goka AK, Alexander GJ, Williams RS. Increased plasma tumor necrosis factor in severe alcoholic hepatitis. Ann Intern Med 1990;112:917–20.
[8] Gonzalez-Amaro R, Garcia-Monzon C, Garcia-Buey L, Moreno-Otero R, Alonso JL, Yague E, et al. Induction of tumor necrosis factor alpha production by human hepatocytes in chronic viral hepatitis. J Exp Med 1994;179:841–8.
[9] Bradham CA, Plumpe J, Manns MP, Brenner DA, Trautwein C. Mechanisms of hepatic toxicity. I. TNF-induced liver injury. Am J Physiol 1998;275: G387–92.
[10] McClain CJ, Song Z, Barve SS, Hill DB, Deaciuc I. Recent advances in alcoholic liver disease. IV. Dysregulated cytokine metabolism in alcoholic liver disease. Am J Physiol Gastrointest Liver Physiol 2004;287:G497–502.
[11] Menon KV, Stadheim L, Kamath PS, Wiesner RH, Gores GJ, Peine CJ, et al. A pilot study of the safety and tolerability of etanercept in patients with alcoholic hepatitis. Am J Gastroenterol 2004;99:255–60.
[12] Carroll MB, Bond MI. Use of tumor necrosis factor-alpha inhibitors in patients with chronic hepatitis B infection. Semin Arthritis Rheum 2008, in press.
[13] Keane J, Gershon S, Wise RP, Mirabile-Levens E, Kasznica J, Schwieterman WD, et al. Tuberculosis associated with infliximab, a tumor necrosis factor alpha-neutralizing agent. N Engl J Med 2001;345:1098–104.
[14] Shakoor N, Michalska M, Harris CA, Block JA. Drug-induced systemic lupus erythematosus associated with etanercept therapy. Lancet 2002;359:579–80.
[15] Aggarwal BB, Eessalu TE, Hass PE. Characterization of receptors for human tumour necrosis factor and their regulation by gamma-interferon. Nature 1985;318:665–7.
[16] Wajant H, Pfizenmaier K, Scheurich P. Tumor necrosis factor signaling. Cell Death Differ 2003;10:45–65.
[17] MacEwan DJ. TNF receptor subtype signalling: differences and cellular consequences. Cell Signal 2002;14:477–92.
[18] Bradley J. TNF-mediated inflammatory disease. J Pathol 2008;214:149–60.
[19] Yamamoto Y, Tsutsumi Y, Yoshioka Y, Nishibata T, Kobayashi K, Okamoto T, et al. Site-specific PEGylation of a lysine-deficient TNF-alpha with full bioactivity. Nat Biotechnol 2003;21:546–52.
[20] Shibata H, Yoshioka Y, Ikemizu S, Kobayashi K, Yamamoto Y, Mukai Y, et al. Functionalization of tumor necrosis factor-alpha using phage display technique and PEGylation improves its antitumor therapeutic window. Clin Cancer Res 2004;10:8293–300.
[21] Shibata H, Yoshioka Y, Ohkawa A, Minowa K, Mukai Y, Abe Y, et al. Creation and X-ray structure analysis of the tumor necrosis factor receptor-1-selective mutant of a tumor necrosis factor-alpha antagonist. J Biol Chem 2008;283:998–1007.
[22] Vandenabeele P, Declercq W, Vanhaesebroeck B, Grooten J, Fiers W. Both TNF receptors are required for TNF-mediated induction of apoptosis in PC60 cells. J Immunol 1995;154:2904–13.
[23] Recknagel RO, Glende Jr EA, Dolak JA, Waller RL. Mechanisms of carbon tetrachloride toxicity. Pharmacol Ther 1989;43:139–54.
[24] Tiegs G, Hentschel J, Wendel A. A T cell-dependent experimental liver injury in mice inducible by concanavalin A. J Clin Invest 1992;90:196–203.
[25] Mizuhara H, O'Neill E, Seki N, Ogawa T, Kusunoki C, Otsuka K, et al. T cell activation-associated hepatic injury: mediation by tumor necrosis factors and protection by interleukin 6. J Exp Med 1994;179:1529–37.
[26] Wolf AM, Wolf D, Rumpold H, Ludwiczek S, Enrich B, Gastl G, et al. The kinase inhibitor imatinib mesylate inhibits TNF-{alpha} production in vitro and prevents TNF-dependent acute hepatic inflammation. Proc Natl Acad Sci USA 2005;102:13622–7.
[27] Bruccoleri A, Gallucci R, Germolec DR, Blackshear P, Simeonova P, Thurman RG, et al. Induction of early-immediate genes by tumor necrosis factor alpha contribute to liver repair following chemical-induced hepatotoxicity. Hepatology 1997;25:133–41.
[28] Yamada Y, Fausto N. Deficient liver regeneration after carbon tetrachloride injury in mice lacking type 1 but not type 2 tumor necrosis factor receptor. Am J Pathol 1998;152:1577–89.
[29] Kita H, Mackay IR, Van De Water J, Gershwin ME. The lymphoid liver: considerations on pathways to autoimmune injury. Gastroenterology 2001;120:1485–501.
[30] Heneghan MA, McFarlane IG. Current and novel immunosuppressive therapy for autoimmune hepatitis. Hepatology 2002;35:7–13.
[31] Lohr HF, Schlaak JF, Lohse AW, Bocher WO, Arenz M, Gerken G, et al. Autoreactive CD4+ LKM-specific and anticlonotypic T-cell responses in LKM-1 antibody-positive autoimmune hepatitis. Hepatology 1996;24:1416–21.
[32] Rothe J, Lesslauer W, Lotscher H, Lang Y, Koebel P, Kontgen F, et al. Mice lacking the tumour necrosis factor receptor 1 are resistant to TNF-mediated toxicity but highly susceptible to infection by Listeria monocytogenes. Nature 1993;364:798–802.
[33] Nowak M, Gaines GC, Rosenberg J, Minter R, Bahjat FR, Rectenwald J, et al. LPS-induced liver injury in D-galactosamine-sensitized mice requires secreted TNF-alpha and the TNF-p55 receptor. Am J Physiol Regul Integr Comp Physiol 2000;278:R1202–9.
[34] Grell M, Douni E, Wajant H, Lohden M, Clauss M, Maxeiner B, et al. The transmembrane form of tumor necrosis factor is the prime activating ligand of the 80 kDa tumor necrosis factor receptor. Cell 1995;83:793–802.
[35] Kusters S, Tiegs G, Alexopoulou L, Pasparakis M, Douni E, Kunstle G, et al. In vivo evidence for a functional role of both tumor necrosis factor (TNF) receptors and transmembrane TNF in experimental hepatitis. Eur J Immunol 1997;27:2870–5.
[36] Alexopoulou L, Pasparakis M, Kollias G. A murine transmembrane tumor necrosis factor (TNF) transgene induces arthritis by cooperative p55/p75 TNF receptor signaling. Eur J Immunol 1997;27:2588–92.
[37] Yoshioka Y, Tsutsumi Y, Nakagawa S, Mayumi T. Recent progress on tumor missile therapy and tumor vascular targeting therapy as a new approach. Curr Vasc Pharmacol 2004;2:259–70.
[38] Mukai Y, Yoshioka Y, Tsutsumi Y. Phage display and PEGylation of therapeutic proteins. Comb Chem High Throughput Screen 2005;8:145–52.

Journal of Immunological Methods 335 (2008) 71–78

Contents lists available at ScienceDirect

Journal of Immunological Methods

journal homepage: www.elsevier.com/locate/jim

Research paper

Simple and highly sensitive assay system for TNFR2-mediated soluble- and transmembrane-TNF activity

Yasuhiro Abe [a,b], Tomoaki Yoshikawa [a,c], Haruhiko Kamada [a,d], Hiroko Shibata [a,e], Tetsuya Nomura [a,b], Kyoko Minowa [a,f], Hiroyuki Kayamuro [a,b], Kazufumi Katayama [g], Hiroyuki Miyoshi [h], Yohei Mukai [a,b], Yasuo Yoshioka [a,c], Shinsaku Nakagawa [b], Shin-ichi Tsunoda [a,d,*], Yasuo Tsutsumi [a,b,d]

[a] *Laboratory of Pharmaceutical Proteomics, National Institute of Biomedical Innovation, 7-6-8 Saito-Asagi, Ibaraki, Osaka 567-0085, Japan*
[b] *Graduate School of Pharmaceutical Sciences, Osaka University, 1-6 Yamadaoka, Suita, Osaka 565-0871, Japan*
[c] *The Center for Advanced Research and Education in Drug Discovery and Development, Osaka University, 1-6 Yamadaoka, Suita, Osaka 565-0871, Japan*
[d] *The Center for Advanced Medical Engineering and Informatics, Osaka University, 1-6 Yamadaoka, Suita, Osaka 565-0871, Japan*
[e] *Division of Drugs, National Institute of Health Science, 1-18-1 Kamiyoga, Setagaya-ku, Tokyo 158-8501, Japan*
[f] *Graduate School of Pharmaceutical Sciences, Kyoto Pharmaceutical University, Misasagi-Nakauchicho 5, Yamashina-ku, Kyoto 607-8414, Japan*
[g] *Allergy & Immunology Project, Tokyo Metropolitan Institute of Medical Science, 3-18-22, Honkomagome, Bunkyo-ku, Tokyo 113-8613, Japan*
[h] *Subteam for Manipulation of Cell Fate, BioResource Center, RIKEN, 3-1-1 Koyadai, Tsukuba, Ibaraki 305-0074, Japan*

ARTICLE INFO

Article history:
Received 25 December 2007
Received in revised form 28 February 2008
Accepted 28 February 2008
Available online 26 March 2008

Keywords:
TNF
TNFR2
Fas
Chimeric receptor
Bioassay

ABSTRACT

Drugs that target tumor necrosis factor-α (TNF) are particularly important in the treatment of severe inflammatory progression in rheumatoid arthritis, Crohn's disease and psoriasis. Despite the central role of the TNF/TNF receptor (TNFR) in various disease states, there is a paucity of information concerning TNFR2 signaling. In this study, we have developed a simple and highly sensitive cell-death based assay system for analyzing TNFR2-mediated bioactivity that can be used to screen for TNFR2-selective drugs. Using a lentiviral vector, a chimeric receptor was engineered from the extracellular and transmembrane domain of human TNFR2 and the intracellular domain of mouse Fas and the recombinant protein was then expressed in TNFR1$^{-/-}$ R2$^{-/-}$ mouse preadipocytes. Our results demonstrate that this chimeric receptor is capable of inducing apoptosis by transmembrane- as well as soluble-TNF stimuli. Moreover, we found that our bioassay based on cell death phenotype had an approximately 80-fold higher sensitivity over existing bioassays. We believe our assay system will be an invaluable research tool for studying TNFR2 and for screening TNFR2-targeted drugs.

1. Introduction

Tumor necrosis factor-α (TNF) is a pleiotropic cytokine that regulates various biological processes such as host defense, inflammation, autoimmunity, apoptosis and tumor cell death through the TNF-receptor 1 (TNFR1) and receptor 2 (TNFR2) (Wajant et al., 2003). TNF/TNFR interaction is considered to be an attractive target for the treatment of refractory diseases, including autoimmune disease and malignant tumors (Aggarwal, 2003; Szlosarek and Balkwill, 2003). In rheumatoid arthritis, for example, biological anti-TNF agents, such as Infliximab and Adalimumab, rapidly reduce signs and symptoms of joint inflammation (Feldmann and Maini, 2003). However, anti-TNF drugs used to treat inflammatory disorders have been reported to increase the risk of infection, in accordance with animal studies (Brown et al., 2002; Nathan et al., 2006).

* Corresponding author. Laboratory of Pharmaceutical Proteomics, National Institute of Biomedical Innovation, 7-6-8 Saito-Asagi, Ibaraki, Osaka 567-0085, Japan. Tel.: +81 72 641 9811x2327; fax: +81 72 641 9817.
E-mail address: tsunoda@nibio.go.jp (S. Tsunoda).

0022-1759/$ – see front matter © 2008 Elsevier B.V. All rights reserved.
doi:10.1016/j.jim.2008.02.019

A thorough understanding of the biology of the TNF/TNFR system is a prerequisite to the safe and effective development of anti-TNF therapeutics. In particular, several factors and mechanisms hypothesized to be involved in the side effects elicited by anti-TNF drugs need to be tested (Curtis et al., 2007; Jacobs et al., 2007; Schneeweiss et al., 2007). These include the differential power of the drugs to neutralize TNF bioavailability and the differential inhibition of TNF signaling events. Despite extensive studies on the molecular biology of TNF/TNFR1 signaling (Micheau and Tschopp, 2003) the functions of TNFR2 are poorly understood. There is an increasing need for a comprehensive understanding of TNF/TNFR2 biology, particularly in terms of the development of TNFR-selective drugs.

In this context, we have used a novel phage-display based screening system (Yamamoto et al., 2003; Shibata et al., 2004, 2008) to develop structural mutants of TNF to help clarify the biology of TNF/TNFR2 interactions. These TNF variants, which exert TNFR2-mediated agonistic or antagonistic activity, might be extremely valuable for elucidating structure-activity relationships between TNF and TNFR2. So far, in order to evaluate the bioactivity of TNF through TNFR2, many researchers have used the TNFR2 over-expressing cell lines (Heller et al., 1992; Weiss et al., 1998), such as rat/mouse T hybridomas transfected with human TNFR2 (PC60-hR2) (Vandenabeele et al., 1992). The PC60-hR2 assay is based on granulocyte macrophage colony-stimulating factor (GM-CSF) secretion mediated by TNF/TNFR2 stimuli. The GM-CSF secretion level is quantified by proliferation of GM-CSF-dependent cell lines or by ELISA. However, this two-step assay system is complicated and the screening process is highly laborious. Thus, there are increasing demands for the development of a simple, highly sensitive screening system that is TNFR2-selective.

In the present study, we developed a simple but highly sensitive cell death-based assay system for evaluating TNFR2-mediated activity. We constructed a lentiviral vector expressing a chimeric receptor derived from the extracellular (EC) and transmembrane (TM) domain of human TNFR2 (hTNFR2) and the intracellular (IC) domain of mouse Fas (mFas). Additionally, to eliminate the influence of the endogenous TNFR1, the chimeric receptor was expressed on TNFR1$^{-/-}$R2$^{-/-}$ preadipocytes (Xu et al., 1999). We found that hTNFR2/mFas-expressing preadipocyte (hTNFR2/mFas-PA) showed about 80-times higher sensitivity after treatment with soluble-TNF and over the conventional method. Furthermore, hTNFR2/mFas-PA could detect not only transmembrane TNF- (tmTNF) but also soluble TNF-activity. The technology described herein will be highly useful both as an assay system for various TNF variants *via* TNFR2 and also as a cell-based drug discovery system for TNFR2 agonists/antagonists.

2. Materials and methods

2.1. Cell culture

TNFR1$^{-/-}$R2$^{-/-}$, TNFR1$^{-/-}$, and wild-type (wt) preadipocytes established from day 16–17 mouse embryos were generously provided by Dr. Hotamisligil (Harvard School of Public Health, Boston MA). Preadipocytes, 293T cells and HeLaP4 cells were cultured in Dulbecco's modified Eagle's medium (DMEM; Sigma-Aldrich, Inc., Tokyo, Japan) with 10% bovine fetal serum (FBS) and 1% antibiotic cocktail (penicillin 10,000 u/ml, streptomycin 10 mg/ml, and amphotericin B 25 μg/ml; Nacalai Tesque, Kyoto, Japan). The rat/mouse T hybridomas PC60-hR2 cells (hTNFR2 transfected PC60 cells) were generously provided by Dr. Vandenabeele (University of Gent, Belgium) and cultured in RPMI 1640 (Sigma-Aldrich, Inc.) with 10% FBS, 1 mM sodium pyrubate, 5×10^{-5} M 2-ME, 3 μg/ml puromycin (Wako Pure Chemical Industries, Osaka, Japan), and 1% antibiotic cocktail. TNFR1$^{-/-}$R2$^{-/-}$ mouse macrophages were generously provided by Dr. Aggarwal (University of Texas MD Anderson Cancer Center, Houston, TX), and cultured in RPMI 1640 with 10% FBS and 1% antibiotic cocktail.

2.2. Construction of self-inactivating (SIN) lentiviral vector

Vectors were constructed using standard cloning procedures. A DNA fragment encoding the EC and TM parts of hTNFR2 was amplified by polymerase chain reaction (PCR) from human peripheral blood lymphocyte cDNA with the following primer pairs: forward primer (5′-GAT TAC GCC AAG CTT GTC GAC CAC CAT GGC GCC CGT CGC CGT CTG GGC CGC GCT GGC CGT CGG ACT GGA G-3′) containing a SalI site at the 5′-end and a reverse primer (5′-CAC CTT GGC TTC TCT CTG CTT TCG AAG GGG CTT CTT TTT CAC CTG GGT CA-3′) containing a Csp45I site. The resulting amplified fragment was subcloned into pCR-Blunt II-TOPO (Invitrogen Corp., Carlsbad, CA) to generate pCR-Blunt-hTNFR2. A fragment encoding the IC domain of mFas was amplified by PCR from mouse spleen cDNA with the following primer pair: forward primer (5′-AAT TCC ACT TGT ATT TAT ACT TCG AAA GTA CCG GAA AAG A-3′) containing a Csp45I site and a reverse primer (5′-GTC ATC CTT GTA GTC TGC GGC CGC TCA CTC CAG ACA TTG TCC TTC ATT TTC ATT TCC A-3′) containing a NotI site at the 5′-end. The mFas DNA fragment was subcloned into pCR-Blunt-hTNFR2 between the Csp45I and NotI sites to combine the EC and TM domains of hTNFR2 to the IC domains of mFas, generating pCR-Blunt-hTNFR2/mFas (Fig. 1A). Then the hTNFR2/mFas DNA fragment was cloned between the XhoI and NotI sites of SIN lentiviral vector construct, which contains the blasticidin (Bsd) resistance gene, generating CSII-CMV-hTNFR2/mFas-IRES2-Bsd (Fig. 1B). For construct tmTNF, a DNA fragment encoding non-cleavable human tmTNF h(tmTNFΔ1-12), generated by deleting amino acids 1–12 in the N-terminal part of hTNF, was amplified by PCR from hTNF cDNA with following primer pair: forward primer (5′-AGT GAT CGG CCC CCA GAG GGA AGC TTA GAT CTC TCT CTA ATC AGC CCT CTG GCC CAG GCA GTA GCC CAT GTT GTA GCA AAC CCT CAA G-3′) and reverse primer (5′-GGT TGG ATG TTC GTC CTC CGC GGC CGC CTA ACT AGT TCA CAG GGC AAT GAT CCC AAA GTA GAC CTG-3′) and cloned into the pY03′ vector. Then tmTNFΔ1–12 DNA fragment was cloned between the SalI and XhoI sites of the SIN vector construct, generating CSII-EF-tmTNF-IRES-GFP.

2.3. Preparation of lentiviral vectors

The method used to prepare the lentiviral vector has been described previously (Miyoshi et al., 1999; Katayama et al.,

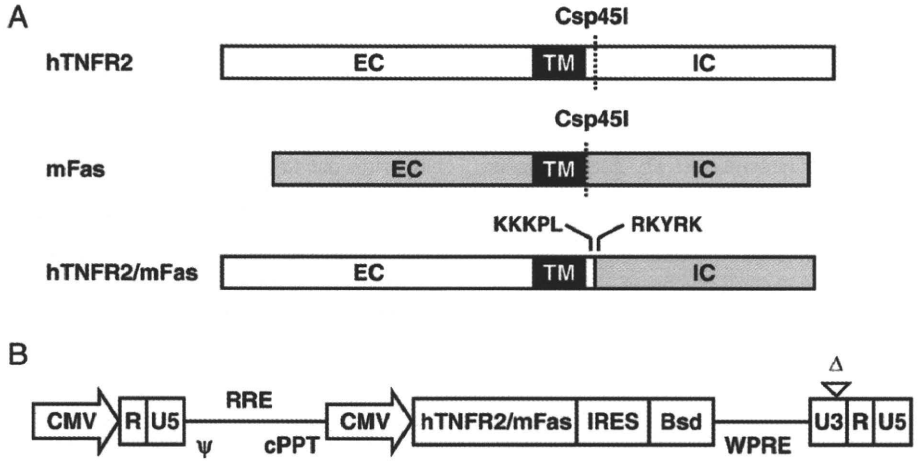

Fig. 1. Construction of hTNFR2/mFas chimeric receptor gene and vector. (A) The cDNA structures of hTNFR2, mFas and fusion genes (hTNFR2/mFas) are shown. EC: extracellular domain, TM: transmembrane domain, IC: Intracellular domain. (B) Schematic representation of self-inactivating (SIN) LV plasmid (CSII-CMV-hTNFR2/mFas-IRES-Bsd). CMV, cytomegalovirus promoter; ψ: packaging signal; RRE, rev responsive element; cPPT, central polypurine tract; IRES, Encephalomyocarditis virus internal ribosomal entry site; Bsd, Blasticidin; WPRE, woodchuck hepatitis virus posttranscriptional regulatory element. Δ: deleting 133 bp in the U3 region of the 3′ long terminal repeat.

2004). In brief, 293T cells were transfected by the calcium phosphate method with three plasmids: packaging construct (pCAG-HIVgp), VSV-G and Rev expressing construct (pCMV-VSV-G-RSV-Rev) and SIN vector construct (CSII-CMV-TNFR2/Fas-IRES2-Bsd or CSII-EF-tmTNF-IRES-GFP). Two days after transfection, the conditioned medium was collected and the virus was concentrated by ultracentrifugation at 50,000 × *g* for 2 h at 20 °C. The pelleted virus was resuspended in Hanks' balanced salt solution (GIBCO BRL, Paisley, UK). Vector titers were determined by measuring the infectivity of HeLaP4 cells with serial dilutions of vector stocks using flow cytometric analysis (FCM) for hTNFR2/mFas- or GFP-positive cells.

2.4. Preparation of hTNFR2/mFas- or tmTNF-expressing cell culture

To prepare the hTNFR2/mFas- or tmTNF-expressing cell culture, $TNFR1^{-/-}R2^{-/-}$ preadipocytes or $TNFR1^{-/-}R2^{-/-}$ macrophages were infected with each lentiviral vector at a multiplicity of infection (MOI) of 100. Stable hTNFR2/mFas-transfectants were selected for growth in culture medium containing 8 μg/ml Bsd (Invitrogen Corp.) for 1 week. Expression of hTNFR2/mFas chimeric receptor on Bsd-resistant cells was detected by staining with biotinylated anti-hTNFR2 antibody (BD Biosciences, Franklin Lakes, NJ) at 0.5 μg/5×10^5 cells for 30 min at 4 °C. Subsequently, the cells were washed and stained with streptavidin-PE conjugate (BD Biosciences). The cell suspension was centrifuged at 800 × g, washed with PBS, centrifuged again, and then re-suspended in 500 μl of 0.4% paraformaldehyde. Fluorescence was analyzed on a FACS Vantage flow cytometer, and data were analyzed using CellQuest software (both BD Biosciences). The hTNFR2/mFas-positive cell cultures were used in subsequent experiments as hTNFR2/mFas-PA cells. For preparation of tmTNF-expressing $TNFR1^{-/-}R2^{-/-}$ macrophages (tmTNF-Mφ), IRES-driven GFP positive cells were sorted by FACSAria (BD Biosciences).

2.5. Cytotoxicity assays

Cells were seeded on 96-well micro titer plates at a density of 1.5×10^4 cells/well in culture medium. Serial dilutions of mouse or human TNF (mTNF or hTNF; Peprotech, Rocky Hill, NJ), anti-mFas antibody (clone Jo2; BD Biosciences), or paraformaldehyde-fixed tmTNF-Mφ were prepared with DMEM containing 1 μg/ml cycloheximide, and added to each well. After 48 h incubation, the cell viability was measured by WST-8 assay kit (Nacalai Tesque) according to the manufacturer's instructions. The assay is based on cleavage of the tetrazolium salt WST-8 to formazan by cellular mitochondrial dehydrogenase.

2.6. Induction of GM-CSF secretion on PC60-hR2

5×10^4 of PC60-hR2 cells were seeded on a 96 well plate and then exposed to a serial dilution of hTNF in the presence of IL-1β (2 ng/ml). After 24 h incubation, hTNFR2-mediated GM-CSF secretion on PC60-hR2 cells was quantified by ELISA kit according to the manufacturer's protocol (R&D Systems, Minneapolis, MN).

2.7. Immunoprecipitation and western blotting

For immunoprecipitation we used FLAG-TNF (a FLAG-tag fusion protein of hTNF), which was generated in *E. coli* and purified in our laboratory. The protocol for the expression and purification of recombinant proteins has been described previously (Yamamoto et al., 2003). 1×10^7 hTNFR2/mFas-PA cells were treated with or without 100 ng/ml of FLAG-TNF for 30 min at 37 °C. Cells were then harvested and lysed in 1 ml of lysis buffer (50 mM Tris HCl, pH 7.4, 150 mM NaCl, 1% Triton X-100, 1 mM EDTA and protease inhibitor cocktail; Sigma-Aldrich Inc.) and gently rocked at 4 °C for 30 min. Cell debris was removed by centrifugation at 10,000 ×g for 30 min. The resulting supernatant was immunoprecipitated with anti-FLAG-M2 affinity beads (Sigma, St.Louis, MO) for 4 h at 4 °C. Immune complexes bound to the beads were washed three

times with 500 μl of lysis buffer and eluted with 3×FLAG peptide at a concentration of 150 ng/ml. Collected proteins were resolved on 10–20% SDS-PAGE gels and transferred to polyvinylidene fluoride membranes (Millipore Corp., Billerica, MA) by electroblotting. Western blot analyses were performed with biotinylated anti-hTNFR2 antibody (R&D systems) or anti-FADD (Fas-associated death domain protein) antibody (H-181; Santa Cruz Biotechnology Inc., Santa Cruz, CA). Bound primary antibodies were visualized with horseradish peroxidase-conjugated streptavidin or goat–anti-rabbit-IgG (Jackson Immunoresearch Lab., West Grove, PA) respectively, and ECL plus western blotting detection reagents (GE Healthcare, Buckinghamshire, UK). A LAS 3000 image analyzer (Fujifilm, Tokyo, Japan) was used for the observation of chemiluminescence.

3. Results

3.1. Fas- but not TNFR-mediates induction of cell-death in $TNFR1^{-/-}R2^{-/-}$ preadipocytes

Initially, we established a cell line that could be used to evaluate TNFR2-specific bioactivity by means of the chimeric receptor (hTNFR2/mFas) strategy. The parental cell line must

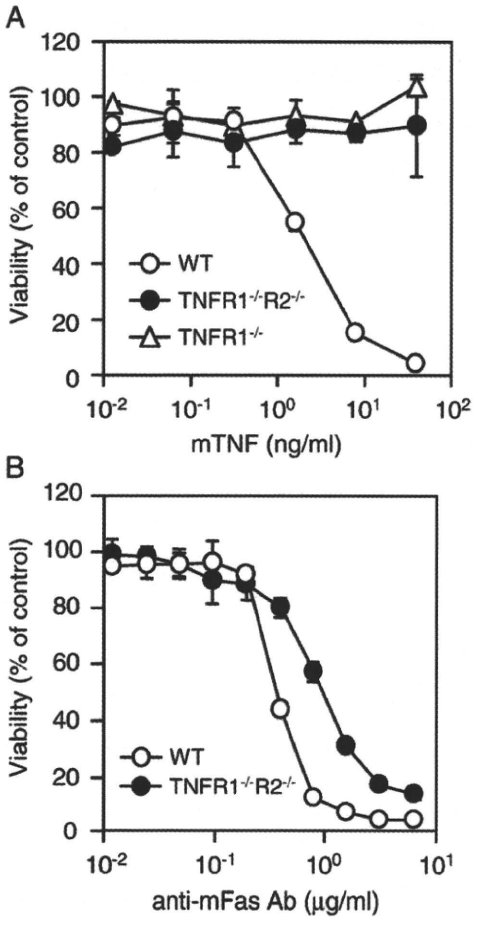

Fig. 2. Fas, but not TNFR2, induced cell death in preadipocytes. WT, $TNFR1^{-/-}R2^{-/-}$ and $TNFR1^{-/-}$ cells were treated with serial dilutions of (A) mTNF or (B) anti-mFas Ab. Cell viability was determined using the WST-8 Assay. Each data point represents the mean±SD of triplicate wells.

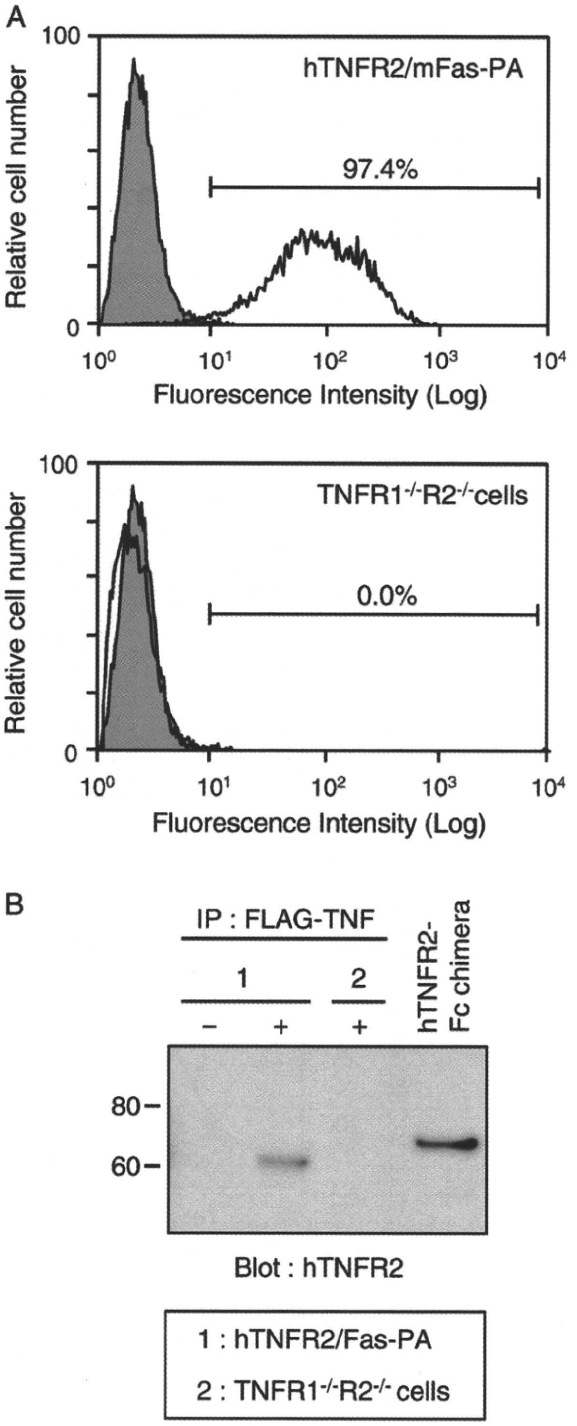

Fig. 3. Expression of hTNF2/mFas chimeric receptor on transfectants. (A) Expression of the chimeric receptor on hTNFR2/mFas-PA (upper panel) or parental $TNFR1^{-/-}R2^{-/-}$ cells (lower panel) was analyzed by flow cytometry using hTNFR2-specific antibody (open histograms) or isotype control antibody (shaded histograms). (B) hTNFR2/mFas-PA or $TNFR1^{-/-}R2^{-/-}$ cells were treated (+) with FLAG-TNF; (−) denotes untreated control cells. Immunoprecipitation was performed with anti-FLAG antibody M2-conjugated beads. After extensive washing, the immunocomplexes were eluted with 3×FLAG peptide. Eluted proteins were resolved on 10–20% SDS-PAGE gels and the presence of hTNFR2/mFas in the complex was detected by western blot using anti-hTNFR2 antibody.

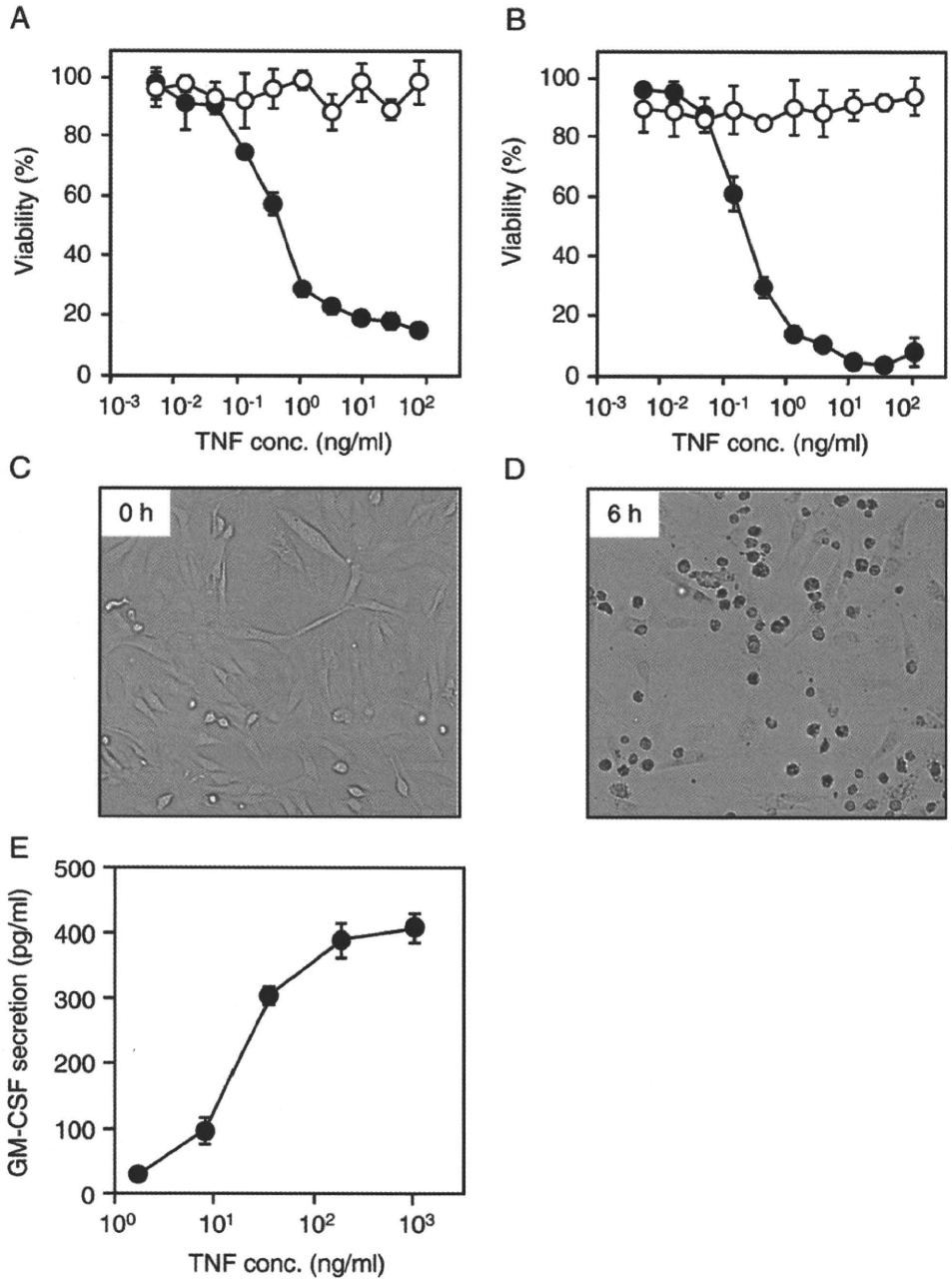

Fig. 4. Induction of strong cell death on hTNFR2/mFas-PA by soluble hTNF. hTNFR2/mFas-PA (●) and parental TNFR1$^{-/-}$R2$^{-/-}$ (○) cells were treated with serial dilutions of hTNF in the presence of cycloheximide (1 μg/ml). After (A) 24 h and (B) 48 h, the cell viability was measured using the WST-8 Assay. Data from the WST-8 assay represents the mean and SDs of triplicate assays. Similar results were obtained in three independent experiments. (C) Untreated or (D) hTNF-treated (10 ng/ml) hTNFR2/mFas-PA cells were incubated for 6 h, and were assessed by light microscopy. (E) PC60-hR2 cells were incubated in the presence of a serial dilution of hTNF and IL-1β (2 ng/ml). After 24 h, induction of GM-CSF was determined by ELISA. Each data point represents the mean±SD of triplicate measurements.

possess both Fas-sensitivity and TNF-resistance. Thus, we selected TNFR1$^{-/-}$R2$^{-/-}$ preadipocytes as the parental cell line and then examined the susceptibility of this cell line against TNFR1- and Fas-induced cell death. TNFR1$^{-/-}$R2$^{-/-}$ preadipocytes were resistant to TNF-induced cell death, while WT preadipocytes, which co-express both TNFR1 and TNFR2, were killed by mTNF-treatment in a dose-dependent manner (Fig. 2A). TNFR1$^{-/-}$ preadipocytes were also resistant to TNF-induced cell death. Thus, TNF-mediated cell death is presumably due to TNFR1-stimuli in accordance with previous reports (Vandenabeele et al., 1995; Ashkenazi and Dixit, 1998; Devin et al., 2000). Anti-Fas antibody treatment induced cell death for both WT, R1$^{-/-}$ and TNFR1$^{-/-}$R2$^{-/-}$ preadipocytes (Fig. 2B). Based on these results, we therefore selected TNFR1$^{-/-}$R2$^{-/-}$ preadipocytes for constructing an hTNFR2/mFas-expressing cell line.

3.2. hTNFR2-expression analysis of LV-hTNFR2/mFas-Bsd infected Bsd-resistant cells

Using the LV technique followed by Bsd selection, we established transfectants that stably expressed hTNFR2/mFas chimeric receptor in which the EC and TM portion of hTNFR2 (amino acids 1–292) was fused to the IC region of mFas (amino acids 187–328) (Figs. 1A and B). FCM analysis revealed that almost 95% of Bsd-resistant cells expressed the EC domain of hTNFR2 (Fig. 3A). To determine whether hTNFR2/mFas retained binding activity against hTNF, we next performed immunoprecipitation and western blot analysis (Fig. 3B). These analyses showed that FLAG-TNFs were immunoprecipitated and eluted with hTNFR2/mFas from LV-transfected and Bsd-resistant cells, but not from parental TNFR1$^{-/-}$R2$^{-/-}$ preadipocytes and untreated cells. Thus, we succeeded in constructing hTNFR2/mFas expressing TNFR1$^{-/-}$ R2$^{-/-}$ preadipocytes that retained the ability to bind hTNF.

3.3. Induction of apoptosis on hTNFR2/mFas-PA

To examine whether the death signal could be transduced by stimulating the chimeric receptors, we evaluated the cell viability of soluble hTNF-treated hTNFR2/mFas-PA. As anticipated, addition of hTNF to hTNFR2/mFas-PA induced a strong cytotoxic effect 24 and 48 h later, whereas no cell death was detected using parental TNFR1$^{-/-}$R2$^{-/-}$ preadipocytes (Figs. 4A and B). After 48 h, more than 90% of hTNFR2/mFas-PA cells were killed by hTNF at a concentration of 4 ng/ml, resulting in a median effective concentration (EC50) of 250 pg/ml. The images in Figs. 4C and D show that hTNFR2/mFas-PA cells underwent clear morphological changes, indicating apoptosis by hTNF stimuli. Additionally, PC60-hR2 cells were tested for hTNFR2-mediated GM-CSF secretion (Fig. 4E). The concentration required to induce 50% of maximal secretion of GM-CSF obtained with hTNF (EC50) was approximately 20 ng/ml. Importantly, our bioassay based on cell death phenotype displayed a ~80-fold higher level of sensitivity over conventional methodologies. Moreover, tmTNF (Fig. 5) and anti-TNFR2 agonistic antibody (data not shown) induced hTNFR2/mFas-PA cell death.

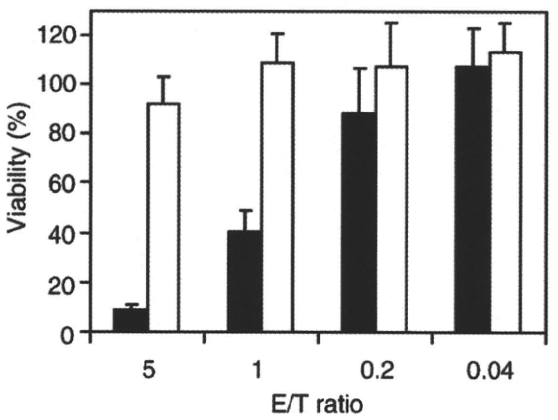

Fig. 5. hTNFR2/mFas-PA cells could be induced cell death by tmTNF. hTNFR2/mFas-PA cells were co-incubated with paraformaldehyde-fixed tmTNF-Mϕ (filled bars) or TNFR1$^{-/-}$R2$^{-/-}$ Mϕ (open bars) at an effector/target (E/T) ratio of 5:1, 1:1, 0.2:1 and 0.4:1 in the presence of cycloheximide (1 μg/ml). After 48 h, cell viability was measured by WST-8 Assay. Each data point represents the mean ± SD of triplicate measurements.

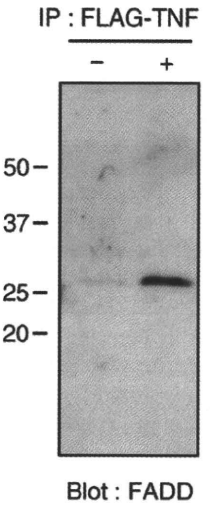

Fig. 6. Recruitment of FADD to the hTNFR2/mFas chimeric receptor in response to hTNF. hTNFR2/mFas-PA or TNFR1$^{-/-}$R2$^{-/-}$ cells were treated (+) with FLAG-TNF; (–) denotes untreated cells. Immunoprecipitation was performed with anti-FLAG antibody M2-conjugated beads. After extensive washing, immunocomplexes were eluted with 3 × FLAG peptide. The eluted proteins were resolved on 10–20% SDS-PAGE gels and the presence of hTNFR2/mFas in the complex was detected by western blot using anti-FADD Antibody.

3.4. Recruitment of FADD to the hTNFR2/mFas chimeric receptor

Recent studies indicate that some TNFR family members, including Fas, self-associate as trimers prior to ligand binding. Activation of the pre-associated receptors is triggered by ligand-induced rearrangement of the assembled trimers (Algeciras-Schimnich et al., 2002). We speculated that the first reaction after ligand-induced oligomerization of hTNFR2/mFas might be the recruitment of FADD, leading to caspase-8 activation. To investigate the composition of the ligand-hTNFR2/mFas signaling complex, we treated hTNFR2/mFas-PA cells with FLAG-tagged hTNF and affinity purified the receptor complex using anti-FLAG antibody-conjugated beads, followed by western blot analysis with antibody against FADD. As expected, FADD was immunoprecipitated with hTNFR2/mFas on hTNF-treated hTNFR2/mFas-PA (Fig. 6). In similar experiments, we could not detect TRADD, which is recruited to TNFR1 in a ligand-dependent process (data not shown). It has been reported that, in contrast to TNFR1, Fas does not interact with TRADD but directly recruits FADD, leading to efficient cell death (Stanger et al., 1995; Dempsey et al., 2003). Because hTNFR2/mFas interacts with FADD, our hTNFR2/mFas-PA cell-based assay system will be useful for evaluating hTNF activity specifically *via* hTNFR2.

4. Discussion

Here, we developed a hTNFR2/mFas-PA cell-based assay system in order to investigate hTNF activity through hTNFR2. The assay is simple to perform and can detect hTNF-mediated hTNFR2 activity with high sensitivity. Because the hTNFR2/

mFas-PA system was engineered in TNFR1$^{-/-}$R2$^{-/-}$ preadipocytes, we were able to analyze hTNF-mediated hTNFR2 activity without affecting TNFR1-related apoptosis. Moreover, not only tmTNF- but also soluble TNF-mediated hTNFR2 activity was detectable using the hTNFR2/mFas-PA cell system.

In our system, hTNFR2-mediated cytotoxic activity on hTNFR2/mFas-PA cells was quantitatively determined using the WST-8 assay. Alternative methods, such as the MTT assay or Methylene Blue assay, are also capable of detecting cytotoxicity. Using the WST-8 assay, hTNFR2-mediated cytotoxic activity was readily detected 24 h after hTNF treatment (Fig. 4A), although a stronger signal was generated with a longer incubation time (48 h; Fig. 4B). Therefore, 48 h-treatment might be more appropriate for evaluating the activity of a low dose of hTNF or when analyzing an activity-weakened mutant TNF. Furthermore, if you evaluate in the absence of CHX, it may be desirable to alter the cell numbers from 1.5 to 1.0×10^4 cells/well. Previously, a similar assay system to the one described in this report was developed by Heidenreich et al. based on murine TNFR1$^{-/-}$R2$^{-/-}$ cells, which heterogenetically expressed human Fas conjugated with hTNFR2 (termed MF-R2-Fas cells) (Krippner-Heidenreich et al., 2002). However, there are some important differences between the MF-R2-Fas cells and the cell line used in our assay system (hTNFR2/mFas-PA), such as detachability. Surprisingly, unlike MF-R2-Fas cells, hTNFR2/mFas-PA cells can detect tmTNF-mediated activity as well as soluble TNF activity. Currently, the reason for this difference is unclear, although it may be caused by heterogeneity of the Fas domain. Indeed, the genetic homology between murine Fas and human Fas in IC domain is approximately 50%. Additionally, other factors may account for the observed differences between the two assay systems, such as expression level of the chimeric receptor. At any event, our results suggest that hTNFR2/mFas-PA cells will be useful in providing the basis for a highly sensitive assay system for analyzing hTNFR2 activity mediated by both soluble TNF and tmTNF. We are currently attempting to generate a TNFR2-selective mutant TNF using this assay system and a phage display system for TNF-therapy or anti-TNF therapy (unpublished data). We chose to use hTNFR2/mFas-PA cells in the screening process for a TNFR2-selective mutant TNF because this cell line is sensitive against not only purified TNF but also culture supernatants of TNF-transfected *E. coli* (crude samples). Therefore, our simple and sensitive bioassay enables high-throughput screening for TNFR2-selective mutant TNFs. The TNFR2-selective mutant will make it possible to perform a structure-function study of TNF/TNFR at any stage of function.

With the success of the human genome project, the focus of life science research has shifted to functional and structural analyses of proteins, such as disease proteomics (Oh et al., 2004; Gilchrist et al., 2006). Thus, there is increasing expectation on drug discovery/development based on the information from genomics or proteomics research, structural biology studies, or receptor-ligand interaction analyses. In particular, the therapeutic application of bioactive proteins, such as cytokines and the newly identified ligand proteins, is eagerly awaited (Gollob et al., 2003; Ansell et al., 2006). Surprisingly, however, these ligand proteins display multiple functions, which has severely limited their clinical application (Margolin et al., 1994; Eskander et al., 1997). Because the reason behind this limitation is that these ligand proteins stimulate different signal transduction pathways via multiple (two or more) receptors, the discovery of receptor-specific agonistic or antagonistic drugs is keenly awaited. Our assay system using a chimeric receptor strategy is applicable to other cytokines and thereby provides a new avenue for identifying receptor-specific agonists or antagonists. We fully anticipate that our novel technology will accelerate the development of TNFR2-related therapeutic molecules as well as acting as a research tool for studying the biology of TNFR2.

Acknowledgements

This study was supported in part by Grants-in-Aid for Scientific Research (No. 18015055, 17689008) from the Ministry of Education, Culture, Sports, Science and Technology of Japan, in part by Health Labor Sciences Research Grant from the Ministry of Health, Labor and Welfare of Japan, in part by Health Sciences Research Grants for Research on Health Sciences focusing on Drug Innovation from the Japan Health Sciences Foundation, and in part by JSPS Research Fellowships for Young Scientists from the Japan Society for the Promotion of Science.

References

Aggarwal, B.B., 2003. Signalling pathways of the TNF superfamily: a double-edged sword. Nat. Rev. Immunol. 3, 745.

Algeciras-Schimnich, A., Shen, L., Barnhart, B.C., Murmann, A.E., Burkhardt, J.K., Peter, M.E., 2002. Molecular ordering of the initial signaling events of CD95. Mol. Cell Biol. 22, 207.

Ansell, S.M., Geyer, S.M., Maurer, M.J., Kurtin, P.J., Micallef, I.N., Stella, P., Etzell, P., Novak, A.J., Erlichman, C., Witzig, T.E., 2006. Randomized phase II study of interleukin-12 in combination with rituximab in previously treated non-Hodgkin's lymphoma patients. Clin. Cancer Res. 12, 6056.

Ashkenazi, A., Dixit, V.M., 1998. Death receptors: signaling and modulation. Science 281, 1305.

Brown, S.L., Greene, M.H., Gershon, S.K., Edwards, E.T., Braun, M.M., 2002. Tumor necrosis factor antagonist therapy and lymphoma development: twenty-six cases reported to the Food and Drug Administration. Arthritis Rheum. 46, 3151.

Curtis, J.R., Patkar, N., Xie, A., Martin, C., Allison, J.J., Saag, M., Shatin, D., Saag, K.G., 2007. Risk of serious bacterial infections among rheumatoid arthritis patients exposed to tumor necrosis factor alpha antagonists. Arthritis Rheum. 56, 1125.

Dempsey, P.W., Doyle, S.E., He, J.Q., Cheng, G., 2003. The signaling adaptors and pathways activated by TNF superfamily. Cytokine Growth Factor Rev. 14, 193.

Devin, A., Cook, A., Lin, Y., Rodriguez, Y., Kelliher, M., Liu, Z., 2000. The distinct roles of TRAF2 and RIP in IKK activation by TNF-R1: TRAF2 recruits IKK to TNF-R1 while RIP mediates IKK activation. Immunity 12, 419.

Eskander, E.D., Harvey, H.A., Givant, E., Lipton, A., 1997. Phase I study combining tumor necrosis factor with interferon-alpha and interleukin-2. Am. J. Clin. Oncol. 20, 511.

Feldmann, M., Maini, R.N., 2003. Lasker Clinical Medical Research Award. TNF defined as a therapeutic target for rheumatoid arthritis and other autoimmune diseases. Nat. Med. 9, 1245.

Gilchrist, A., Au, C.E., Hiding, J., Bell, A.W., Fernandez-Rodriguez, J., Lesimple, S., Nagaya, H., Roy, L., Gosline, S.J., Hallett, M., Paiement, J., Kearney, R.E., Nilsson, T., Bergeron, J.J., 2006. Quantitative proteomics analysis of the secretory pathway. Cell 127, 1265.

Gollob, J.A., Veenstra, K.G., Parker, R.A., Mier, J.W., McDermott, D.F., Clancy, D., Tutin, L., Koon, H., Atkins, M.B., 2003. Phase I trial of concurrent twice-weekly recombinant human interleukin-12 plus low-dose IL-2 in patients with melanoma or renal cell carcinoma. J. Clin. Oncol. 21, 2564.

Heller, R.A., Song, K., Fan, N., Chang, D.J., 1992. The p70 tumor necrosis factor receptor mediates cytotoxicity. Cell 70, 47.

Jacobs, M., Togbe, D., Fremond, C., Samarina, A., Allie, N., Botha, T., Carlos, D., Parida, S.K., Grivennikov, S., Nedospasov, S., Monteiro, A., Le Bert, M.,

Quesniaux, V., Ryffel, B., 2007. Tumor necrosis factor is critical to control tuberculosis infection. Microbes Infect. 9, 623.

Katayama, K., Wada, K., Miyoshi, H., Ohashi, K., Tachibana, M., Furuki, R., Mizuguchi, H., Hayakawa, T., Nakajima, A., Kadowaki, T., Tsutsumi, Y., Nakagawa, S., Kamisaki, Y., Mayumi, T., 2004. RNA interfering approach for clarifying the PPARgamma pathway using lentiviral vector expressing short hairpin RNA. FEBS Lett. 560, 178.

Krippner-Heidenreich, A., Tubing, F., Bryde, S., Willi, S., Zimmermann, G., Scheurich, P., 2002. Control of receptor-induced signaling complex formation by the kinetics of ligand/receptor interaction. J. Biol. Chem. 277, 44155.

Margolin, K., Aronson, F.R., Sznol, M., Atkins, M.B., Gucalp, R., Fisher, R.I., Sunderland, M., Doroshow, J.H., Ernest, M.L., Mier, J.W., et al., 1994. Phase II studies of recombinant human interleukin-4 in advanced renal cancer and malignant melanoma. J. Immunother. Emphas. Immunol. 15, 147.

Micheau, O., Tschopp, J., 2003. Induction of TNF receptor I-mediated apoptosis via two sequential signaling complexes. Cell 114, 181.

Miyoshi, H., Smith, K.A., Mosier, D.E., Verma, I.M., Torbett, B.E., 1999. Transduction of human CD34+ cells that mediate long-term engraftment of NOD/SCID mice by HIV vectors. Science 283, 682.

Nathan, D.M., Angus, P.W., Gibson, P.R., 2006. Hepatitis B and C virus infections and anti-tumor necrosis factor-alpha therapy: guidelines for clinical approach. J. Gastroenterol. Hepatol. 21, 1366.

Oh, P., Li, Y., Yu, J., Durr, E., Krasinska, K.M., Carver, L.A., Testa, J.E., Schnitzer, J.E., 2004. Subtractive proteomic mapping of the endothelial surface in lung and solid tumours for tissue-specific therapy. Nature 429, 629.

Schneeweiss, S., Setoguchi, S., Weinblatt, M.E., Katz, J.N., Avorn, J., Sax, P.E., Levin, R., Solomon, D.H., 2007. Anti-tumor necrosis factor alpha therapy and the risk of serious bacterial infections in elderly patients with rheumatoid arthritis. Arthritis Rheum. 56, 1754.

Shibata, H., Yoshioka, Y., Ikemizu, S., Kobayashi, K., Yamamoto, Y., Mukai, Y., Okamoto, T., Taniai, M., Kawamura, M., Abe, Y., Nakagawa, S., Hayakawa, T., Nagata, S., Yamagata, Y., Mayumi, T., Kamada, H., Tsutsumi, Y., 2004. Functionalization of tumor necrosis factor-alpha using phage display technique and PEGylation improves its antitumor therapeutic window. Clin. Cancer Res. 10, 8293.

Shibata, H., Yoshioka, Y., Ohkawa, A., Minowa, K., Mukai, Y., Abe, Y., Taniai, M., Nomura, T., Kayamuro, H., Nabeshi, H., Sugita, T., Imai, S., Nagano, K., Yoshikawa, T., Fujita, T., Nakagawa, S., Yamamoto, A., Ohta, T., Hayakawa, T., Mayumi, T., Vandenabeele, P., Aggarwal, B.B., Nakamura, T., Yamagata, Y., Tsunoda, S., Kamada, H., Tsutsumi, Y., 2008. Creation and X-ray structure analysis of the tumor necrosis factor receptor-1-selective mutant of a tumor necrosis factor-alpha antagonist. J. Biol. Chem. 283, 998.

Stanger, B.Z., Leder, P., Lee, T.H., Kim, E., Seed, B., 1995. RIP: a novel protein containing a death domain that interacts with Fas/APO-1 (CD95) in yeast and causes cell death. Cell 81, 513.

Szlosarek, P.W., Balkwill, F.R., 2003. Tumour necrosis factor alpha: a potential target for the therapy of solid tumours. Lancet Oncol. 4, 565.

Vandenabeele, P., Declercq, W., Beyaert, R., Fiers, W., 1995. Two tumour necrosis factor receptors: structure and function. Trends Cell Biol. 5, 392.

Vandenabeele, P., Declercq, W., Vercammen, D., Van de Craen, M., Grooten, J., Loetscher, H., Brockhaus, M., Lesslauer, W., Fiers, W., 1992. Functional characterization of the human tumor necrosis factor receptor p75 in a transfected rat/mouse T cell hybridoma. J. Exp. Med. 176, 1015.

Wajant, H., Pfizenmaier, K., Scheurich, P., 2003. Tumor necrosis factor signaling. Cell Death Differ. 10, 45.

Weiss, T., Grell, M., Siemienski, K., Muhlenbeck, F., Durkop, H., Pfizenmaier, K., Scheurich, P., Wajant, H., 1998. TNFR80-dependent enhancement of TNFR60-induced cell death is mediated by TNFR-associated factor 2 and is specific for TNFR60. J. Immunol. 161, 3136.

Xu, H., Sethi, J.K., Hotamisligil, G.S., 1999. Transmembrane tumor necrosis factor (TNF)-alpha inhibits adipocyte differentiation by selectively activating TNF receptor 1. J. Biol. Chem. 274, 26287.

Yamamoto, Y., Tsutsumi, Y., Yoshioka, Y., Nishibata, T., Kobayashi, K., Okamoto, T., Mukai, Y., Shimizu, T., Nakagawa, S., Nagata, S., Mayumi, T., 2003. Site-specific PEGylation of a lysine-deficient TNF-alpha with full bioactivity. Nat. Biotechnol. 21, 546.

doi:10.1016/j.jmb.2008.11.053 J. Mol. Biol. (2009) 385, 1221–1229

JMB

Available online at www.sciencedirect.com

ScienceDirect

ELSEVIER

Structure–Function Relationship of Tumor Necrosis Factor (TNF) and Its Receptor Interaction Based on 3D Structural Analysis of a Fully Active TNFR1-Selective TNF Mutant

Yohei Mukai[1,2], Hiroko Shibata[2], Teruya Nakamura[3], Yasuo Yoshioka[2,4], Yasuhiro Abe[2], Tetsuya Nomura[1,2], Madoka Taniai[5], Tsunetaka Ohta[5], Shinji Ikemizu[3], Shinsaku Nakagawa[1], Shin-ichi Tsunoda[2], Haruhiko Kamada[2], Yuriko Yamagata[3] and Yasuo Tsutsumi[1,2]*

[1]*Graduate School of Pharmaceutical Sciences, Osaka University, 1-6 Yamadaoka, Suita, Osaka 565-0871, Japan*

[2]*Laboratory of Pharmaceutical Proteomics, National Institute of Biomedical Innovation, Osaka 567-0085, Japan*

[3]*Graduate School of Pharmaceutical Sciences, Kumamoto University, Kumamoto 862-0973, Japan*

[4]*The Center for Advanced Research and Education in Drug Discovery and Development, Osaka University, 1-6 Yamadaoka, Suita, Osaka 565-0871, Japan*

[5]*Hayashibara Biochemical Laboratories, Inc., 1-2-3 Shimoishii, Okayama 702-8006, Japan*

Received 9 July 2008; received in revised form 21 November 2008; accepted 22 November 2008
Available online 6 December 2008

Edited by I. Wilson

Tumor necrosis factor (TNF) is an important cytokine that suppresses carcinogenesis and excludes infectious pathogens to maintain homeostasis. TNF activates its two receptors [TNF receptor (TNFR) 1 and TNFR2], but the contribution of each receptor to various host defense functions and immunologic surveillance is not yet clear. Here, we used phage display techniques to generate receptor-selective TNF mutants that activate only one TNFR. These TNF mutants will be useful in the functional analysis of TNFR.

Six amino acids in the receptor binding interface (near TNF residues 30, 80, and 140) were randomly mutated by polymerase chain reaction. Two phage libraries comprising over 5 million TNF mutants were constructed. By selecting the mutants without affinity for TNFR1 or TNFR2, we successfully isolated 4 TNFR2-selective candidates and 16 TNFR1-selective candidates, respectively. The TNFR1-selective candidates were highly mutated near residue 30, whereas TNFR2-selective candidates were highly mutated near residue 140, although both had conserved sequences near residues 140 and 30, respectively. This finding suggested that the phage display technique was suitable for identifying important regions for the TNF interaction with TNFR1 and TNFR2. Purified clone R1-6, a TNFR1-selective candidate, remained fully bioactive and had full affinity for TNFR1 without activating TNFR2, indicating the usefulness of the R1-6 TNF mutant in analyzing TNFR1 receptor function.

To further elucidate the receptor selectivity of R1-6, we examined the structure of R1-6 by X-ray crystallography. The results suggested that R31A and R32G mutations strongly influenced electrostatic interaction with TNFR2, and that L29K mutation contributed to the binding of R1-6 to TNFR1. This phage display technique can be used to efficiently construct functional mutants for analysis of the TNF structure–function relationship, which might facilitate *in silico* drug design based on receptor selectivity.

Keywords: TNF; X-ray crystallography; phage display system; TNF mutant; receptor specificity

**Corresponding author.* Department of Toxicology, Graduate School of Pharmaceutical Sciences, Osaka University, 1-6 Yamadaoka, Suita, Osaka 565-0871, Japan. E-mail address: ytsutsumi@phs.osaka-u.ac.jp.

Abbreviations used: TNF, tumor necrosis factor; TNFR, TNF receptor; SPR, surface plasmon resonance; wtTNF, wild-type TNF; PDB, Protein Data Bank.

Introduction

Tumor necrosis factor (TNF) is as an important immunity-modulating cytokine that is required for human body defense against infectious diseases and carcinogenesis.[1] Excess TNF, however, causes various autoimmune diseases, such as rheumatoid arthritis, Crohn's disease, and ulcerative colitis.[2–4] The relationship between TNF and disease deterioration must be unraveled before effective therapies can be developed. Both TNF receptor (TNFR) types TNFR1 and TNFR2, which induce different cell signaling, must be analyzed to better understand the function of TNF. Experiments with TNFR knockout mice have revealed the individual functions of TNFR1 and TNFR2 against viral infection, microbial pathogens, and tumor immunity.[5–8] The lack of one TNFR type, however, can affect the function of the other receptor type and weaken its signaling because the two receptors work together by crosstalk signaling.[9–11] This issue complicates investigations of the individual roles of TNFR1 and TNFR2, and the analysis of TNFR function. Therefore, many researchers have attempted to activate only one receptor using a receptor-selective TNF mutant that does not impair the function of the receptor.

In the past decade, several receptor-selective TNF mutants, which are useful for functional analysis of TNFRs, have been constructed.[12,13] Traditional point mutation methods, however, are labor-intensive because a large number of candidates must be individually assessed; therefore, it has been difficult to successfully isolate the desired mutants.[14–17] In particular, a receptor-selective TNF mutant with full bioactivity was difficult to develop due to the fact that a region on TNF shares a binding affinity for the two different receptors.[18,19] Furthermore, inadequate mutations cause a loss of affinity for both TNFR1 and TNFR2, which has made it difficult to create novel mutants with high selectivity and full bioactivity.[20] Therefore, functional analysis of TNFR using these mutants has not progressed sufficiently.

We previously developed a modified phage display technique that can be used to create desired functional mutant proteins. Using this technique, we have successfully created many mutants with high bioactivity,[21] high *in vivo* stability,[22] and antagonist activity[23] that are suitable for drug development. The advantage of this method is that it allows us to obtain information about specific functions and associated sequences, which is very useful for determining the structure–function relationship of a specific protein. This information will be useful for improving the design of therapeutic mutants.

In the present study, we used the phage display technique to create novel receptor-selective TNF mutants with full bioactivity. Structural information of the mutants was determined by crystallographic analysis, and structural simulation was used to determine a feasible basis for receptor selectivity. These TNF mutants will be useful tools for analyzing TNFR signaling. An understanding of the structure and sequence of these functional mutants, combined with bioinformatics techniques, can potentially lead to the design of a desired functional protein, peptide, or peptide mimic, and thus accelerate the development of novel strategies for analyzing disease-related proteins, such as TNF, and the development of associated therapies.

Results

Library construction and selection of receptor-selective TNF mutants

To create receptor-specific TNF mutants using our phage display system, we prepared two phage libraries, Libraries I and II. Each library contained six amino acids randomized in a receptor binding site suggested by point mutation analysis and X-ray crystallography (Fig. 1).[16,17,24] For construction of the TNF mutant library, a mutant TNF-Lys(−) gene was used as template for polymerase chain reaction (PCR) mutagenesis.[22] Sequence analysis of randomly selected clones indicated that Libraries I and II contained 8.2×10^6 and 5.6×10^6 independent clones, respectively. For selection from the library, several rounds of affinity panning were performed against human TNFR1 or TNFR2 using BIAcore 3000. Potent binders to TNFR1 or TNFR2 were concentrated in the library through this panning procedure. The monoclonal candidates in each library were picked up for enzyme-linked immunosorbent assay (ELISA) screening to confirm their receptor binding specifi-

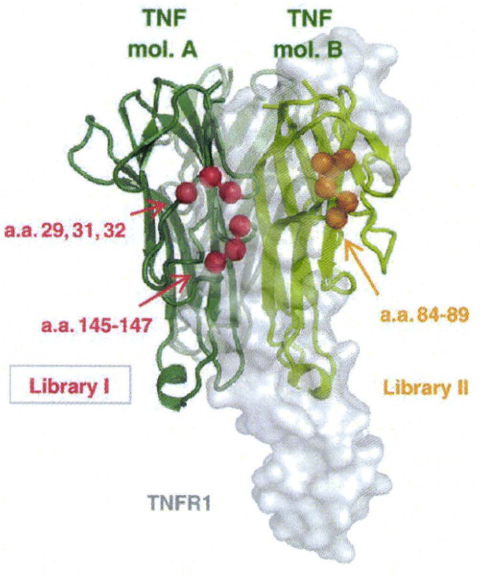

Fig. 1. Positions of randomized residues on the binding interface of the TNF–TNFR1 complex. Mutational residues of Library I (red spheres) and Library II (orange spheres). Green cartoon represents wtTNF. White area represents the surface of the TNFR1 monomer. This binding model structure of the TNF–TNFR1 complex was constructed based on the crystal structure of the LTα–TNFR1 complex (1TNR) and that of wtTNF (1TNF).

Table 1. Substituted residues of TNF mutants from Libraries I and II

			29	31	32	84	85	86	87	88	89	145	146	147
		wtTNF	L	R	R	A	V	S	Y	Q	T	A	E	S
		mutTNF-Lys(−)	—	—	—	—	—	—	—	—	—	—	—	—
TNFR1-selective candidates	Library I (29:32–145:147)	R1-1	I	—	—	—	—	—	—	—	—	—	—	—
		R1-2	Q	—	W	—	—	—	—	—	—	—	—	—
		R1-3	T	G	Y	—	—	—	—	—	—	—	—	—
		R1-4	T	K	Y	—	—	—	—	—	—	—	—	—
		R1-5	T	—	F	—	—	—	—	—	—	—	T	—
		R1-6	K	A	G	—	—	—	—	—	—	—	S	T
	Library II (84:89)	R1-7	—	—	—	S	K	T	—	T	H	—	—	—
		R1-8	—	—	—	S	P	L	—	P	K	—	—	—
		R1-9	—	—	—	S	T	N	—	N	G	—	—	—
		R1-10	—	—	—	T	S	A	—	G	P	—	—	—
		R1-11	—	—	—	T	T	A	—	S	G	—	—	—
		R1-12	—	—	—	T	H	K	—	P	Q	—	—	—
		R1-13	—	—	—	S	K	T	—	S	H	—	—	—
		R1-14	—	—	—	S	S	H	—	R	F	—	—	—
TNFR2-selective candidates	Library I (29:32–145:147)	R2-1	—	—	—	—	—	—	—	—	—	K	D	T
		R2-2	—	—	—	—	—	—	—	—	—	R	T	D
		R2-3	—	—	—	—	—	—	—	—	—	R	E	T
		R2-4	—	—	—	—	—	—	—	—	—	A	D	D
		R2-5	—	—	—	—	—	—	—	—	—	A	N	D

Conserved residues compared with wtTNF are indicated by an em dash (—). Mutated residues in each library are highlighted in gray. Library I included mutated residues 29, 31, 32, and 145–147. Library II contained mutated residues 84–89. R1-1–R1-6 and R1-7–R1-14 were isolated from Libraries I and II, respectively, as TNFR1-selective candidates. TNFR2-selective clones R2-1–R2-5 were isolated from Library I; Library II contained no TNFR2-selective clones.

city. Several clones with TNFR1 or TNFR2 specificity were eventually obtained.

Sequence analysis of receptor-specific TNF mutant candidates

Sequence analysis revealed that we had 14 TNFR1-selective candidates (R1-1–R1-14) and 5 TNFR2-selective candidates (R2-1–R2-5) from Libraries I and II (Table 1). Unfortunately, Library II did not contain any TNFR2-selective mutants. All active TNFR1-selective mutants in Library II retained Tyr87, suggesting that Tyr87 was an essential residue for receptor binding. Analysis of Library I, however, revealed that the mutated and conserved regions of the TNFR1-selective mutants were different from

Table 2. Receptor-selective bioactivities and affinities of TNF mutants

			Relative affinity (% K_d)[a]			Relative bioactivity (% of EC_{50})		
		TNFs	TNFR1	TNFR2	R_1/R_2	HEp2[b]	PC60[c]	R_1/R_2
		wtTNF	100	100	1.0	100	100	1.0
		mutTNF-Lys(−)	108	88	1.2	116	126	0.9
TNFR1-selective candidates	Library I (29:32–145:147)	R1-1	145	121	1.2	492	NT	—
		R1-2	212	32	6.7	436	NT	—
		R1-3	42	18	2.4	343	NT	—
		R1-4	43	3	13.4	447	NT	—
		R1-5	177	2	106.2	582	36	16.2
		R1-6	33	4	8.4	128	<0.07	>1800.0
	Library II (84:89)	R1-7	108	13	8.4	102	NT	—
		R1-8	145	9	16.5	120	173	0.7
		R1-9	175	24	7.4	110	NT	—
		R1-10	149	9	17.0	134	NT	—
		R1-11	219	11	20.4	58	NT	—
		R1-12	51	15	3.5	21	NT	—
		R1-13	51	11	4.6	26	NT	—
		R1-14	46	4	12.0	47	47	1.0
TNFR2-selective candidates	Library I (29:32–145:147)	R2-1	83	112	0.741	12.4	23	0.539
		R2-2	3	143	0.020	0.2	30	0.007
		R2-3	38	225	0.169	2.5	12	0.208
		R2-4	51	572	0.089	6.2	19	0.326
		R2-5	94	324	0.290	13.4	39	0.344

The affinity and bioactivity values are shown as relative values (% wtTNF).
NT, not tested.
[a] Affinity for immobilized TNFR1 and TNFR2 was assessed by SPR using BIAcore 3000.
[b] Human TNFR1-mediated bioactivity was evaluated using a HEp-2 cell cytotoxicity assay. In this assay, HEp-2 cell viability was determined by methylene blue staining. Each value represents the mean±SD.
[c] Human TNFR2-mediated bioactivity was evaluated using PC60-R2 assay. GM-CSF expression by TNFR2-mediated signaling was detected by ELISA. Each value presents the mean±SD.

those of the TNFR2-selective mutants. TNFR1-selective mutants were highly mutated near residue 30 and conserved near residue 140. On the other hand, TNFR2-selective mutants were mutated near residue 140 and conserved near residue 30. This interesting result suggested that the details of the essential binding interface for TNFR1 and TNFR2 differed despite their predicted similar complex forms.[19]

Receptor selectivity and bioactivity of TNF mutants

To investigate the properties of candidate receptor-selective TNF mutants in detail, we prepared recombinant protein using the previously described methods.[21,22] TNF mutants expressed as an inclusion body in *Escherichia coli* were denatured and refolded. Then, active TNF mutants were purified by ion-exchange and gel-filtration chromatography. TNF mutant purity was greater than 90% in sodium dodecyl sulfate–polyacrylamide gel electrophoresis, and all mutants were confirmed to form trimers by gel-filtration analysis (data not shown).

We examined the affinities of these recombinant TNF mutants for TNFR1 and TNFR2 (Table 2). Most of the TNFR1-selective candidates had little affinity for TNFR2 based on surface plasmon resonance (SPR) analysis by BIAcore 3000. In particular, the TNFR1 affinities of R1-2, R1-5, R1-8, R1-9, R1-10, and R1-11 were higher than that of wild-type TNF (wtTNF), despite the loss of their TNFR2 affinities. TNFR1- and TNFR2-mediated bioactivities were assessed by HEp-2 and PC60-hTNFR2 assays, respectively. Interestingly, R1-selective candidates from Library I showed more potent activity via TNFR1 than those from Library II. R1-5 and R1-6 showed superior bioactivity and receptor selectivity. R1-6 was selected as the best overall mutant with greater than 1800-fold selective TNFR1 activity. These mutants were novel because TNFR1-selective mutants with higher bioactivity had not yet been established. Similar studies were performed with the TNFR2-selective candidates. In SPR analysis, these candidates showed higher TNFR2 affinity than wtTNF. Unfortunately, however, none of the TNFR2-selective candidates could sufficiently activate TNFR2 and had less than 40% of the bioactivity of wtTNF.

Next, we performed a competitive binding assay to confirm the details of the TNFR1 selectivity of R1-5 and R1-6—the candidates with the highest selectivity for TNFR1. Competitive affinities were assessed under a certain amount of wtTNF-FLAG, wtTNF fusing FLAG-tag (DYKDDDDK) at C-terminal, as competitor (Fig. 2). Similar to the results of the SPR analysis, R1-5 showed a higher affinity for TNFR1 compared with wild type, and its affinity for TNFR2 was decreased to approximately 10% that for wtTNF, suggesting that R1-5 was a TNFR1-selective mutant. In contrast to the SPR results, however, R1-6 showed a higher competitive affinity for TNFR1, and wtTNF–FLAG binding to TNFR2 was not completely inhibited, even by excess R1-6, which suggested that R1-6

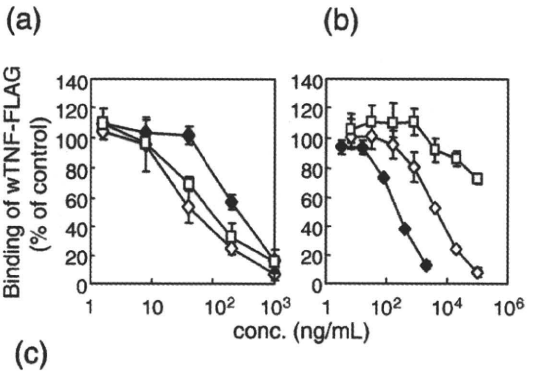

(c)

	TNFR1		TNFR2	
	IC50 (ng/ml)	(%)	IC50 (ngml)	(%)
wtTNF	276.0	100.0	508.1	100.0
R1-5	57.7	478.3	4606.6	11.0
R1-6	105.4	261.9	> 100000.0	< 0.5

Fig. 2. Competitive binding affinities of TNFR1-selective mutants (R1-5 and R1-6). Competitive affinities were assessed under 50 ng/ml FLAG-tagged wtTNF (wtTNF–FLAG) as competitor. Both (a) TNFR1 and (b) TNFR2 were immobilized. Binding of wtTNF–FLAG was inhibited by serially diluted TNF mutants. Final binding of wtTNF–FLAG was assessed by ELISA. Each value represents the mean±SD. (c) IC_{50} values are given as the concentration of the TNF mutant required to inhibit 50% of the maximal binding of wtTNF–FLAG.

lacked binding potency to TNFR2. Because the TNF binding interfaces to the receptors are known to overlap,[19] TNFR1 selectivity caused by a structural change in the R1-6 surface might provide important information for structure-based drug discovery.

X-ray crystallography of TNFR1-selective TNF mutant R1-6

The structural basis of the TNFR1 selectivity of R1-6 was examined by X-ray crystallography. After establishing crystallization conditions, good-quality crystals of R1-6 were obtained (approximately 0.2 mm×0.2 mm×0.3 mm in size). X-ray diffraction data were collected in SPring-8 (a large synchrotron radiation facility in Harima, Japan). Analysis of these data indicated that the space group is *R*3 and that the lattice constants are $a=135.87$ Å, $b=135.87$ Å, and $c=58.02$ Å (Table 3). The R1-6 structure was further refined using the CNS software suite. The results of model validation using the PROCHECK program indicated that there were 86.9% residues in the most favored regions, 13.1% residues in the additionally allowed regions, 0.0% residues in the generously allowed regions, and 0.0% residues in the disallowed regions.

The overall structures of the R1-6 [Protein Data Bank (PDB) code 2ZJC] and wtTNF (PDB code 1TNF) trimers are also similar and superimpose with an rmsd of 1.21 Å for 428 C^{α} atoms (Fig. 3). The structure of

Table 3. Crystallographic parameters and refinement statistics of the R1-6 crystal

Data collection	
Resolution (Å)	50–2.50 (2.59–2.50)
Cell constants (Å)[a]	135.9, 135.9, 58.0
Space group	*R*3
Measured reflections	74,516
Unique reflections	13,445 (1173)
Completeness (%)	99.9 (85.2)
R_{merge} (%)[b]	0.10 (0.53)
$I/\sigma(I)$	28.9 (4.2)
Refinement statistics	
Resolution (Å)	25.67–2.50
Reflections used	12,060
R_{cryst} (%)[c]	20.1
R_{free} (%)[d]	27.2
Completeness (%)	97.1
Atoms	
Protein; water	3338; 59
rmsd from ideality	
Bond lengths (Å); bond angles (°)	0.009; 1.27
Overall *B*-factor (Å^2)	19.7
B-factor rmsd (Å^2)	
Main-chain bonds; side-chain bonds	0.42; 0.77
Main-chain angles; side-chain angles	0.94; 1.48
Ramachandran plot statistics	
Most favored regions (%)	86.9
Additionally allowed regions (%)	13.1
Generously allowed regions (%)	0.0
Disallowed regions (%)	0.0

Values in parentheses are those for the outer shell.

[a] Cell constants are *a*, *b*, and *c*.

[b] $R_{merge} = \sum |I - \langle I \rangle| / \sum \langle I \rangle$, where I is intensity of the observations. R_{merge} in the last shell is high because of the anisotropic mosaicity of the crystal.

[c] $R_{cryst} = \sum ||F_o| - |F_c|| / \sum |F_o|$, where F_o and F_c are the observed and calculated structure factors, respectively.

[d] R_{free} is calculated as for R_{cryst}, but for the test set comprising reflections not used in refinement. The overall *B*-factor was calculated after TLS parameter analysis (TLSANL) using Refmac.

each monomer is similar to each other (rmsd of 0.98–1.12 Å for 140 C^α atoms). Especially, the structures of the β-sheet in each monomer are essentially the same (rmsd of 0.31–0.42 Å for 63 C^α atoms). These features have been found in the wtTNF trimer.[25]

The R1-6 loop structure near mutational residues 31 and 32 is different from that in wtTNF (Fig. 4). This loop structure between monomers is not different (wtTNF: rmsd of 0.61–0.72 Å for 11 C^α atoms; R1-6: rmsd of 0.39–0.91 Å for 11 C^α atoms) (Fig. 4a and b). However, they are clearly different between wtTNF and R1-6 (Fig. 4c). This structural change is thought to be caused by R32G mutation from a sterically bulky arginine residue to a flexible glycine residue. Because this region is close to the TNFR surface, such a structural change in the C^α chain could influence receptor binding. Additional TNF–TNFR docking simulation studies are discussed below.

Discussion

We recently developed the technology to create functional mutant proteins with high bioactivity, high *in vivo* stability, and antagonistic activity.[21–23] Here, we attempted to establish fully bioactive receptor-selective TNF mutants for functional analysis of TNFR1 and TNFR2 using our optimized phage display system. We constructed TNF mutant libraries (Libraries I and II) in which six residues near the receptor binding region were randomized (Fig. 1). From these libraries, we screened for TNFR1- or TNFR2-selective binders, and isolated receptor-selective candidates (Table 1). Despite the successful isolation of TNFR2-selective binders, the TNFR2-selective candidates obtained could not sufficiently activate TNFR2. This result suggested that the production of TNFR2-selective mutants was very rare in our library and that an improved panning method was necessary.

One advantage of our phage-display-based technique is that it can be used to obtain the sequence information of many mutants (Table 1). Tyr87 of TNF was conserved in all mutants obtained from Library II. This residue is highly conserved throughout the TNF superfamily, such as in LTα, LTβ, and LIGHT, and site-directed mutagenesis of the Tyr87 residue of TNF results in a dramatic loss of its biologic activity and its affinities for both TNFR1 and TNFR2.[17] In addition, Tyr87 replacement in antagonistic TNF causes unstable receptor binding and loss of receptor activation in our report.[23] These findings together indicate that Tyr87 is an essential residue for receptor signaling and receptor complex stability.

TNFR1-selective mutants had mutations near residue 30 and conserved residues near residue 140. In contrast, TNFR2-selective mutants had mutations near residue 140 and conserved residues near residue 30. These findings support those of previous point mutation analyses[15–17] and suggest that our phage-

Fig. 3. Overall structure of wtTNF and R1-6. Merge image of previously reported wtTNF structure (green; 1TNF) and refined structure of R1-6 (white; 2ZJC). The flexible loop containing residues 100–110 shown at the bottom of the figure was disordered in the R1-6 structure.

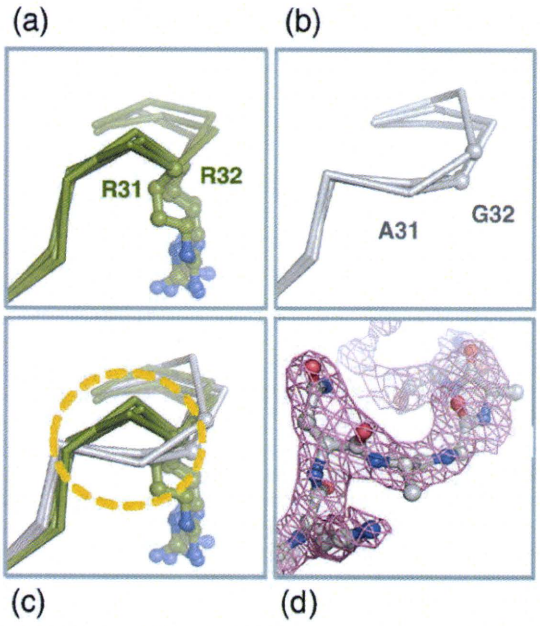

Fig. 4. Structural difference in receptor binding loop between wtTNF and R1-6. Each TNF monomer was superimposed using the CCP4i program. Details of the receptor binding loop, including residues 31 and 32, are shown in these figures. (a) Loops of wtTNF monomers (green); (b) loops of R1-6 monomers (white); (c) merged image of the loops of wtTNF and R1-6; (d) $2F_o-F_c$ map contoured at 1.0σ of R1-6 loop (pink mesh). The different C^{α} chains are highlighted by the dashed orange circle in (c).

display-based technique can be used to rapidly gather important information about the function–sequence relationships determined by long-term point mutation analysis. In the present study, we successfully isolated mutants that retained TNFR affinity from a huge phage library containing over a million repertoires. Most of the mutants in the library had no TNFR affinity and were therefore discarded through this selection step. This finding may indicate that the mutational residues in these unbound clones diminish TNFR affinity. This method may be useful for examining the function, capability, and sequence–function relationship of unknown cytokines and proteins.

Using these receptor-selective candidates, we expressed recombinant proteins and estimated their bioactivities and affinities for TNFR1 and TNFR2. R1-6, the most highly TNFR1-selective mutant, bound and activated TNFR1 efficiently despite the loss of its affinity for TNFR2. X-ray crystallography of R1-6 revealed that the crystal structure of R1-6 was a trimer (similar to wtTNF), and no other salient differences in the overall structure were observed. Superimposition of wtTNF and R1-6 sequences, however, revealed that the C^{α} of the receptor binding loop near residue 30 was partially different (Fig. 4). This change might influence the receptor binding mode of R1-6. We further used the superimposition program to perform docking simulations with TNF and TNFR1 based on the crystal structure of the LTα–TNFR1 complex (PDB code 1TNR).[18]

Based on the model wtTNF–TNFR1 complex, Arg31 of TNF would interact electrostatically with Glu56 of TNFR1. The main chain of TNF was too close to His69 of TNFR1, however, potentially causing potential steric hindrance (Fig. 5a). On the other hand, a structural change in the loop in R1-6, however, was thought to solve this problem (Fig. 5b). Arg32 of wtTNF associated with Ser72 of TNFR1 (Fig. 5a). In the R1-6 structure, however, this role of Arg32 was thought to be compensated for by Lys29 (Fig. 5b). This speculation was supported by the crystal structure of the LTα–TNFR1 complex.[18] The position of Lys29 in R1-6 corresponded to that of Arg46 in LTα interacting with Ser72 of TNFR1 by hydrogen bonding. This interesting "compensating role of an amino acid" would be difficult to induce using single point mutation methods, which is another advantage of our modified phage display technique.

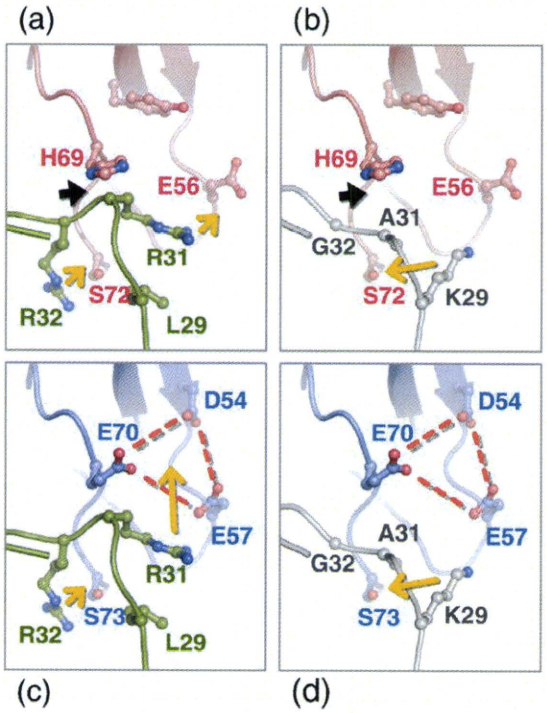

Fig. 5. Model of TNF binding to TNFR1 and TNFR2. Receptor binding interfaces of (a) wtTNF–TNFR1 (green–red); (b) R1-6–TNFR1 (white–red); (c) wtTNF–TNFR2 (green–blue); and (d) R1-6–TNFR2 (white–blue). The TNF–TNFR1 model complex was constructed from 1TNF (wtTNF) and 1TNR (LTα–TNFR1 complex). The predicted TNFR2 structure was constructed by side-chain mutation using the O program. In this simulation, the side chains of each structure were rotated to fit the predicted interaction. Stable structures of these rotamers were constructed using the O program. Steric hindrance might have occurred between His69 of TNFR1 and Arg32 of wtTNF in (a) (black arrowhead). Potential interactions are indicated by orange arrows. A cluster of anionic charged residues (Asp54, Glu57, and Glu70) is highlighted by a broken red line.

Next, we examined the TNFR1 selectivity of R1-6 based on its structure. Because the structure of TNFR2 is thought to be similar to that of TNFR1,[18] we generated a model structure of TNFR2 by manual mutation based on the crystal structure of TNFR1. This TNF–TNFR2 simulation is speculative, but this model, together with the information obtained from previous mutation studies, can be used to form hypotheses regarding the important structural features for TNFR1 selectivity. The binding surface of TNFR2 was composed of Asp54, Glu57, and Glu70, which could cause a strongly negatively charged surface of TNFR2 different from that of TNFR1 (Fig. 5c and d). Arg31 of wtTNF was thought to have an important role in TNFR2 binding by strongly interacting with this surface (Fig. 5c). R1-6 had an R31A mutation, however, which could cause the loss of the affinity of R1-6 for TNFR2 (Fig. 5d). In support of this finding, a single point mutation R31E mutant was previously reported to have a dramatic loss of affinity for TNFR2.[12,14] On the other hand, the R32W mutant is also reported to be a mutant with TNFR1 selectivity.[12] From our library, Arg32 of our TNFR1-selective candidates was replaced with hydrophobic or nonionic amino acids (Trp, Tyr, Phe, and Gly), which might indicate the importance of Arg32 for binding to TNFR2 (Table 1). This structural information, in combination with bioinformatics technology, will be useful for designing more advanced TNFR-selective mutants and TNFR-selective inhibitors (peptide mimics and chemical compounds).

In conclusion, the phage display technique is an attractive method for creating functional mutants, as demonstrated here by the production of TNFR-specific mutants. Application of this method to various cytokines and proteins will enhance the construction of useful receptor-selective mutants and accelerate functional analysis of these proteins. As an advanced application, analysis of the "structure (sequence)–function relationship" using the obtained mutants will be a powerful technique for basic life science research and drug discovery.

Materials and Methods

Cell culture

HEp-2 cells (a human fibroblast cell line) were provided by the Cell Resource Center for Biomedical Research (Tohoku University) and maintained with RPMI 1640 containing 10% fetal bovine serum and antibiotics. PC60-hTNFR2 cells (a mouse–rat fusion hybridoma comprised of human TNFR2-transfected PC60 cells) were provided by Dr. Vandenabeele and maintained in RPMI 1640 supplemented with 10% fetal bovine serum, 1 mM sodium pyruvate, 5×10^{-5} M 2-mercaptoethanol, 3 μg/ml puromycin, and antibiotics (100 U/ml penicillin, 100 μg/ml streptomycin, and 0.25 μg/ml amphotericin B).

Library construction

The pCANTAB phagemid vector (GE Healthcare Ltd., UK) encoding mutTNF-Lys(−) was used as template for PCR. This TNF was previously reported to be a fully active lysine-deficient TNF mutant.[22] Mutations were introduced in TNF at six amino acid codons (Library I: amino acid residues 29, 31, 32, and 145–147; Library II: amino acid residues 84–89) using a two-step PCR. Three primers, Oligos A, B, and C, were used for the construction of Library I. The first PCR was performed using Oligos A and B. The PCR conditions were 5 min at 95 °C, 35 cycles of denaturization at 95 °C for 15 s, and annealing/extension at 68 °C for 2 min. This first PCR product and Oligo C were then annealed to the template, and PCR was performed again under the same conditions. For the construction of Library II, Oligos A, D, and E were used. The first PCR was performed using Oligos A and D. The first PCR product and Oligo E were used as primers for the second PCR. The PCR conditions of Library II were the same as those of Library I. After the second PCR, the PCR products were digested with HindIII and NotI, and then ligated to a pY03′ phagemid vector (modified from pCANTAB) for the display of TNF variants on the phage surface as g3p fusion proteins. The primer sequences used in this experiment are listed below. Oligos A and E were designed to prime to the pCANTAB vector sequence: Oligo A: 5′-GATAACAATTTCACACAGGAAACAGCTATGACCATGATTACGCCAAGCTTTGGAGCC-3′; Oligo B: 5′-CGCCATTGGCCAGGAGGGCATTAGCSNNSNNGTTSNNCCACTGGAGCTGCCCCTCAGCTTGAGGG-3′; Oligo C: 5′-CCAGCGGATCCGGATACGGCACCGGCGCACCTGCGGCCGCGGATCCACCACCACCCAGGGCAATGATCCCAAAGTAGACCTGCCCSNNSNNSNNAAAGTCGAGATAGTCGGGCCGATTGA-3′; Oligo D: 5′-CTGGCAGGGGCTGCGGATGGCAGAGAGGAGATTGACGGGSNNSNNSNNSNNSNNGATGCGGCTGATGGTGTGGGTGAGGAGCAC-3′; Oligo E: 5′-TGCGGCACGCGGTTCCAGCGGATC-3′.

Isolation of receptor-selective TNF mutants from the library (affinity panning and screening)

Human TNFR1 Fc (R&D Systems, Inc., Minneapolis, MN) and TNFR2 Fc (R&D Systems, Inc.) were diluted to 50 μg/ml in 10 mM sodium acetate buffer (pH 4.5) and immobilized on a CM3 sensor chip using an amine coupling kit (GE Healthcare Ltd.), which resulted in an increase of 4000–6000 resonance units. The phage library (1×10^{11} colony-forming units/100 μl) was injected at 3 μl/min over the sensor chip. After binding and until the association phase had been reached, the sensor chip was washed using the rinse command and eluted using 20 μl of 10 mM glycine–HCl. The eluted phage was neutralized with 1 M Tris–HCl (pH 6.9). *E. coli* (TG1) was infected with the collected phage for amplification. This panning cycle was performed two more times. After picking up a single clone of transfected *E. coli*, the phagemid vectors were sequenced using a Big Dye Terminator v3.1 kit and ABI PRISM 3100 (Applied Biosystems Ltd., Pleasanton, CA). After the procedure, the binding affinities of the TNF mutants were assessed by ELISA, and their bioactivities through TNFR1 were determined by cytotoxicity assay in human HEp-2 cells.

Expression and purification of TNF mutants

The protocol for the expression and purification of recombinant protein was the same as that described previously.[21,22] Briefly, TNF mutants were produced in the *E. coli* BL21(DE3) strain. The inclusion body of each

TNF mutant was washed in 2.5% Triton X-100 and solubilized in 6 M guanidine–HCl, 0.1 M Tris–HCl (pH 8.0), and 2 mM ethylenediaminetetraacetic acid. Solubilized protein at 10 mg/ml was reduced with 10 mg/ml dithioerythritol for 4 h at room temperature and refolded by 100-fold dilution in a refolding buffer (100 mM Tris–HCl, 2 mM ethylenediaminetetraacetic acid, 0.5 M arginine, and 551 mg/L oxidized glutathione). After dialysis with 20 mM Tris–HCl (pH 7.4) containing 100 mM urea, active trimeric proteins were purified by ion-exchange chromatography using Q-Sepharose FF (GE Healthcare Ltd.). Size-exclusion chromatography was performed using a Superose 12 column (GE Healthcare Ltd.).

In vitro bioactivity of TNF mutants

HEp-2 cells were used for cytotoxicity assay in the presence of cycloheximide (50 μg/ml). HEp-2 cytotoxicity was dependent on TNFR1 signaling. HEp-2 cells were cultured in 96-well plates in the presence of TNF mutants and serially diluted mouse or human wtTNF (PeproTech EC Ltd., UK) at 4×10^4 cells/well. For neutralization assay, cells were cultured in the presence of a constant concentration of human (20 ng/ml) wtTNF and a serial dilution of TNF mutants. After incubation for 18 h, cell survival was determined by methylene blue assay, as described previously.[21,22] To evaluate the bioactivity of the TNF mutant binding specifically to TNFR2, PC60-hTNFR2 cells were used as an index of granulocyte–macrophage colony-stimulating factor (GM-CSF) production, as described previously.[26] Briefly, PC60-hTNFR2 cells were cultured at 5×10^4 cells/well with interleukin-1β (2 ng/ml) and serially diluted TNF mutant. After 24 h of incubation, the amount of rat GM-CSF produced was quantified by ELISA in accordance with the manufacturer's protocol (R&D Systems, Inc.).

Affinity assessment using SPR

The binding kinetics of wtTNF and TNF mutants were analyzed using the BIAcore 3000 SPR system (GE Healthcare Ltd.). TNFRs were immobilized on a CM5 sensor chip, which resulted in an increase of 3000–5000 resonance units. During the association phase, TNF mutants or wtTNF diluted in HBS-EP running buffer (10 mM HEPES pH7.4, 150 mM NaCl, 3 mM EDTA, 0.005% Tween20, GE Healthcare Ltd.) at 78.4, 26.1, or 8.7 nM were individually passed over the immobilized TNFR at a flow rate of 20 μl/min. During the dissociation phase, HBS-EP buffer was applied to the sensor chip at a flow rate of 20 μl/min. The data were analyzed globally with BIAEVALUATION 3.0 software (GE Healthcare Ltd.) using a 1:1 binding model.

Competitive binding of TNF to TNFR1 and TNFR2 (ELISA)

Goat anti-human IgG (MP Biomedicals, Inc., Solon, OH) was immobilized on Maxisorb 96-well ELISA plates (Nalge Nunc International KK, Japan), and nonspecific binding to the plates was blocked using Block Ace (Dainippon Sumitomo Pharma Co., Ltd., Japan). Human TNFR1-Fc or human TNFR2-Fc (ALEXIS Corporation, Switzerland) was bound to coated antibody. Serially diluted TNF with 50 ng/ml FLAG-tagged wtTNF (wtTNF–FLAG) was added to TNFR1-Fc or TNFR2-Fc in 0.4% Block Ace. wtTNF–FLAG binding was detected by anti-FLAG M2 antibody (Sigma-Aldrich Corporation, St. Louis, MO) and avidin horseradish peroxidase conjugate (Invitrogen Corporation, Carlsbad, CA). The binding affinity of TNF was assessed by competitive wtTNF–FLAG binding to TNFR (IC_{50} value).

X-ray crystallography

Purified R1-6 was concentrated to 10 mg/ml in 20 mM Tris–HCl (pH 7.4). Initial screening using a Hampton Crystal screen 1-2 and Crystal screen Lite kit (Hampton Research Corporation, Aliso Viejo, CA) was performed by vapor diffusion method with hanging drops (1+1 μl) at 20 °C. After optimization of the crystallization conditions, rhombohedral crystals (0.2 mm×0.2 mm×0.3 mm) were obtained with reservoir solution containing 0.5 M ammonium sulfate, 1.2 M lithium sulfate, and 0.1 M trisodium citrate (pH 5.6). The crystals were frozen in a cryopreserving solution containing 15% glycerol as cryoprotectant. X-ray diffraction data to 2.5 Å resolution were collected at BL41XU, SPring-8, under flash cooling to 100 K to reduce the effects of radiation damage. Data integration and scaling were performed using HKL2000.[27] Molecular replacement was performed by the MOLREP program in CCP4i[28] using a crystal structure of the wtTNF (1TNF)[25] as search model. Cycles of manual rebuilding using the O program[29] and refinement using the CNS program[30] led to a refined structure. Final refinement (TLS refinement) was performed using the Refmac program in CCP4i.[28] Final model validation was performed using PROCHECK program in CCP4i.[28] The model complexes of TNF–TNFR1 and R1-6–TNFR1 were constructed based on the crystal structure of the LTα–TNFR1 complex[18] using the superimposing program in CCP4i. Structural models of TNFR2 were constructed based on the TNFR1 structure by manual mutation using the O program.[29]

Accession number

Coordinates and structure factors have been deposited in the PDB with accession number 2ZJC.

Acknowledgements

This study was supported by Research for Promoting Technological Seeds (no. 11-067) from the Japan Science and Technology Agency; Research Fund Project on Health Sciences focusing on Drug Innovation (no. KAA3701) from the Japan Health Sciences Foundation; the Global COE Program "*In Silico* Medicine" (Wakate-16) at Osaka University; a Grant-in-Aid for Young Scientists (B) (no. 20790134) and Grants-in-Aid for Scientific Research (nos. 18015055 and 17689008) from the Ministry of Education, Culture, Sports, Science, and Technology of Japan; and Research Fellowships for Young Scientists (no. 20-3919) from the Japan Society for the Promotion of Science.

References

1. Aggarwal, B. B. (2003). Signalling pathways of the TNF superfamily: a double-edged sword. *Nat. Rev. Immunol.* **3**, 745–756.